UNIVERSITY OF CALIFORNIA,
IRVINE

Validation of Simulated Ground Motions for Bridge Engineering Applications— A Preliminary Study

THESIS

submitted in partial satisfaction of the requirements
for the degree of

MASTER OF SCIENCE

in Civil Engineering

by

Rachelle George Habchi

Thesis Committee:
Professor Farzin Zareian, Chair
Professor Lizhi Sun
Professor Farzad Naeim

2017

DEDICATION

To

my parents

in recognition of the incredible amount of effort they have employed to support me throughout the entirety of my lifetime

and

To

my advisor

in recognition of the copious amount of time dedicated to my academic development and the appreciation of the clever one-liners with double meaning

Life is just a party, and parties weren't meant to last.

Prince Rogers Nelson

TABLE OF CONTENTS

LIST OF FIGURES

LIST OF TABLES

ACKNOWLEDGMENTS

I would like to express the deepest gratitude and appreciation to my committee chair, Professor Farzin Zareian, whose raw intelligence, incredible tenacity, and witty personality are a continual source of inspiration in my professional pursuits. His ability to rapidly understand concepts outside his area of expertise and to provide thought-provoking questions to challenges presented before him are a testament to the level of excellence he achieves as a researcher and a professor. It has been an honor and a privilege to be his student and I thank him for allowing me the opportunity to work with him. Without his guidance and dedication, the research presented herein would have not been possible.

I would like to thank my committee members, Professor Farzad Naeim and Professor Lizhi Sun, whose work in the professional industry and academic community continue are sources of motivation in my professional career.

Financial support was provided in part by the University of California, Irvine, CEE Department Mentor Program Fellowship.

ABSTRACT OF THE THESIS

Validation of Simulated Ground Motions for Bridge Engineering Applications—
A Preliminary Study

By

Rachelle George Habchi

Master of Science in Civil Engineering

University of California, Irvine, 2017

Professor Farzin Zareian, Chair

The study presented herein provides validation of five methodologies (EXSIM, GP, Irikura-Recipe, SDSU, and SONG) for ground motion simulation. The 1994 Northridge earthquake is selected alongside a bridge model as the test bed for this validation. This validation comprises a comparison between Engineering Demand Parameters (EDPs) obtained from Nonlinear Response History Analysis (NLRHA) of the bridge model subject to simulated and recorded motions of Northridge. The significance of the differences between the two EDPs are correlated with Intensity Measures (IMs) of the simulated and recorded motions. The IMs considered are normalized Arias intensity (I_a), Significant Duration (T_d), time at mid-duration (t_{min}), rate of energy accumulation (I_a/T_d), rate of change in predominant frequency (ω'), and predominant frequency at mid duration (ω_{mid}). A regression of logged recorded parameters yielded I_a, T_d, and ω_{mid} as significant IMs. A regression analysis of logged recorded ground motions discovered that ω' was also significant when considering multiple ground motion angles from 0 to 180 at 9˚ increments. A mixed effects regression was performed to establish the influence of simulation realization,

ground motion station, and angle of rotation possessed on the model. Statistical distributions of the recorded and simulated IMs and EDP were compared to each other. Regardless of simulation methodology, the mean and variance of the simulated EDP were comparable to that of the recorded. It is recommended that the methods employed in this study be used with various recorded earthquakes in future research to assess the practicality of this validation approach.

INTRODUCTION

Recordings from naturally occurring earthquakes have been extensively documented in the past couple of decades; however, the quantity of records derived from strong motion shaking, especially those with varying characteristics, are often insufficient in providing statistically meaningful data (Rezaeian, et al. 2015). Simulations of recorded earthquakes with strong ground motions offer a solution to the necessity of a variety of data in engineering applications. Simulated ground motions may be applied in lieu of or as a compliment to recorded ground during performance-based earthquake engineering research and design motions (Somerville, et al. 2001). These simulations may be used as input for nonlinear dynamic analysis in structures (Bozorgnia and Bertero 2004), for generating earthquake intensity measures based off specified parameters (Somerville, et al. 2001), and for designing target performance (Galasso, et al. 2013). Should the use of simulated motions gain in popularity, these applications may have significant impacts in the accuracy of behavior prediction and design of structural systems.

Concerns have been raised about the validity of these simulations as accurate representations of recorded earthquakes in research and in practice. Specifically, the concerns tend to question the ability of the simulations to induce similar behavior in structural response and whether they possess similar statistical parameters to their recorded counterparts.

Figure 1: GM Stations "Northridge." 34 24'08.70" N 118 30'59.04"W. Google Earth

The study presented herein aims to validate the use of simulated ground motions through the comparison of specified intensity measures, the behavior of a two-span bridge, and the statistical distributions of the Intensity Measures (IM) and selected engineering demand parameter (EDP). The recordings used are that of the 1994 Northridge Earthquake, which resulted in wide spread structural failures across the Los Angeles area. The 6.7 M earthquake, which sat on a blind thrust

fault, provided recordings of strong ground motion shaking and has been extensively used for research and design purposes for the past two decades. The ground motion recordings were obtained from 38 ground motion stations. The visual locations of the 38 ground motion stations are depicted in Figure 1. The yellow pins represent the stations and the red pin represents the hypocenter of the event. Each station was numerically re-labeled as stations were assigned numbers (i.e. GM1); the number assignments and their correlating assigned abbreviations are disclosed in Appendix A.

The simulations used were compiled from the USC GMSV website. The simulation methodologies considered were EXSIM, GP, Irikura-Recipe (referred to as IRIK), SDSU, and SONG. Initially, 20 realizations for each simulation methodology were incorporated in the validation analysis. Due to regression results obtained, which are subsequently discussed in depth, it was found that no more than one simulation realization was suitable to be able to meaningfully extrapolate from the data acquired.

CHAPTER 1: Ground Motion Simulation

The current accepted simulation generation methodology incorporates a hybrid broadband approach, in which statistically random probability distributions of simulations and deterministic data are used in high and low frequency parameters, respectively (Graves and Pitarka 2010). Low frequency waves are defined as those with frequencies up to 2 Hz, while high-frequency simulations have frequencies between 2-10 Hz. This combination of stochastic and deterministic simulated data, as Graves and Pitarka (2010) stipulate, is due to the difference in homogeneity in recorded strong ground motions. Lower frequency ground motions tend to be more homogenous, and are more accurately predicted based off specific environmental parameters and event characteristics.

Due to the deterministic nature of low frequency, ground motions, spectral amplitudes as well as recorded waveforms can be accurately captured by predictive models; however, the recorded waveforms prove to be difficult to replicate at higher frequency ground motions (Galasso, et al. 2013). The source of this departure from homogeneity at lower periods, Galasso and Zhong (2013) explicate, is that the source radiation and wave propagation conditions tend towards ambiguity and incoherence. The logical solution to this problem in simulating real-life seismic events is addressed in the arrangement of a simulated hybrid broadband time history. Preliminary construction of the simulated time history accounts for slip distribution and rupture velocity at surface of the fault (Galasso, et al. 2013); subsequent tailoring of the simulated record considers the geologic nonlinear factors for deep-basin amplification and specific amplification for the site in consideration (Campbell and Borzorgnia 2008).

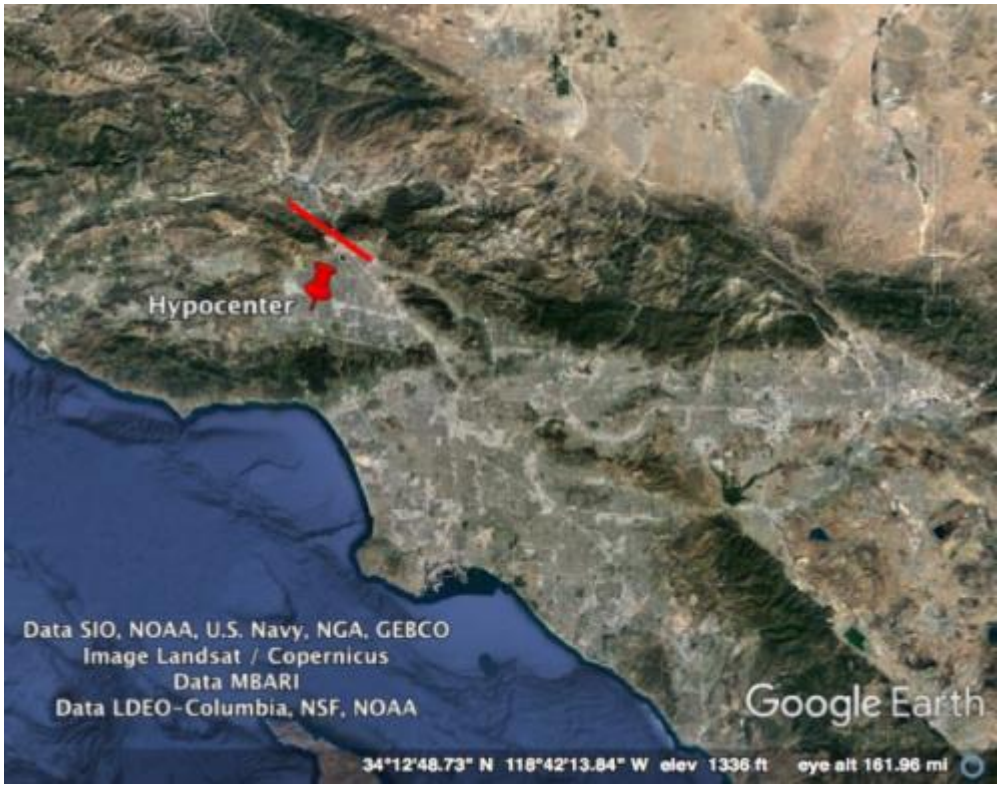

Figure 2: Northridge fault "Northridge." 34 24'08.70" N 118 30'59.04"W. Google Earth

The ground motion prediction equations and corresponding amplification factors, which were developed by Campbell and Borzorgnia are based on the $V_{s,30}$ of the evaluated site; the site coefficients considered herein for the 6.7 Magnitude Northridge earthquake range from 306 m/s at ground motion station 2039-LAN (GM 12) to 2016 m/s at ground motion station 2007-PUL (GM 26) (GMSV_17_3/NR 2017).

Further specifications and parameters used in the simulations of the Northridge earthquake event may be found via the USC research hypocenter simulation website (GMSV_17_3/NR 2017). The fault length, depicted in Figure 2, is 20 meters and the epicenter was taken as 5 meters below ground. Model specific parameters, D_{wid}, D_{len}, and Corner Frequency were taken as 0.1, 0.1, and 0.15, respectively.

CHAPTER 2: Bridge Model

The structural system used to assess the validity of the simulated ground motions is a two-span, one column bridge coded in OpenSees. The point of interest on the bridge, referenced as the chosen EDP, is at the mid height of the cross-section of the deck of the bridge, vertically aligned with the column of the bridge. The point of interest is referred to as Node 12. The displacement of Node 12 in the x and y direction was recorded and the square root of the sum of the squares (SRSS) of the x and y records was taken as the EDP of the bridge. Figure 3 displays a graphic representation of the OpenSees bridge and outlines the specified node used to represent bridge performance.

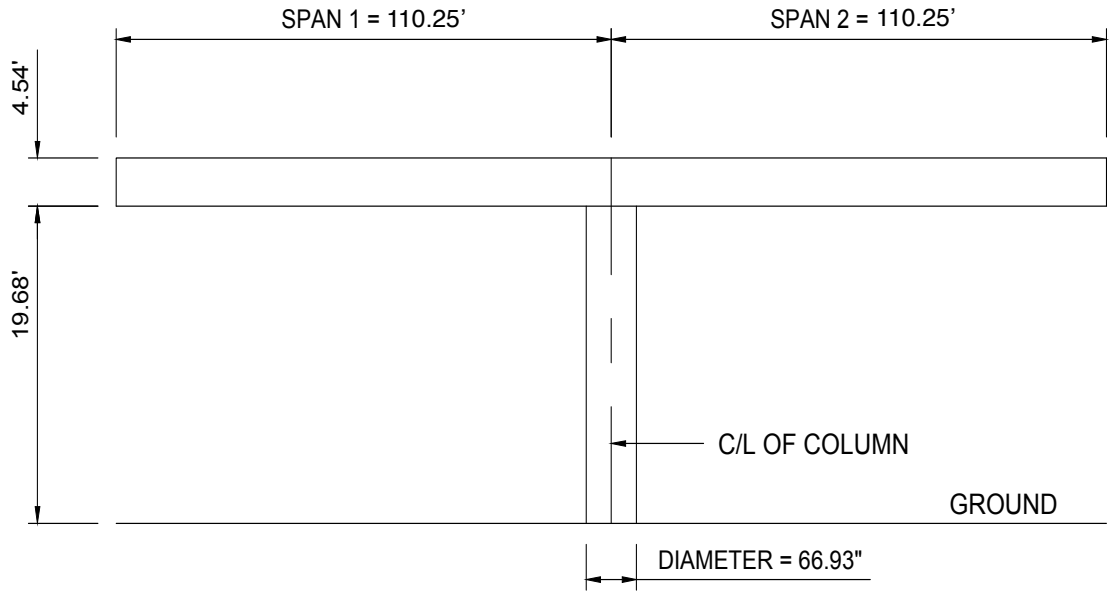

Figure 3: Graphical representation of OpenSees bridge, MATLAB

2.1 Geometrical Characteristics and Material Properties

The OpenSees bridge model used herein was created via (Mobasher 2016). The finite element model bridge is a computer-generated model of the Caltrans Jack Tone Road Overcrossing bridge, which consists of a 22-ft. tall reinforced concrete column supporting two spans of deck. The spans have equal lengths of 110.25 ft. Deep foundation support is provided to the bent column through a group of 25 driven H-piles at 36 feet in height while the abutment skew angle is taken as 33˚ (Mobasher 2016). The deck of the highway bridge consists of cast-in-place concrete and has a width of 27.1 ft. while it's depth is 4.64 ft. The single bent column supporting the two deck spans has a diameter of 5.51 ft. A stick model of the bridge considered via (Mobasher 2016) is displayed below in Figure 4.

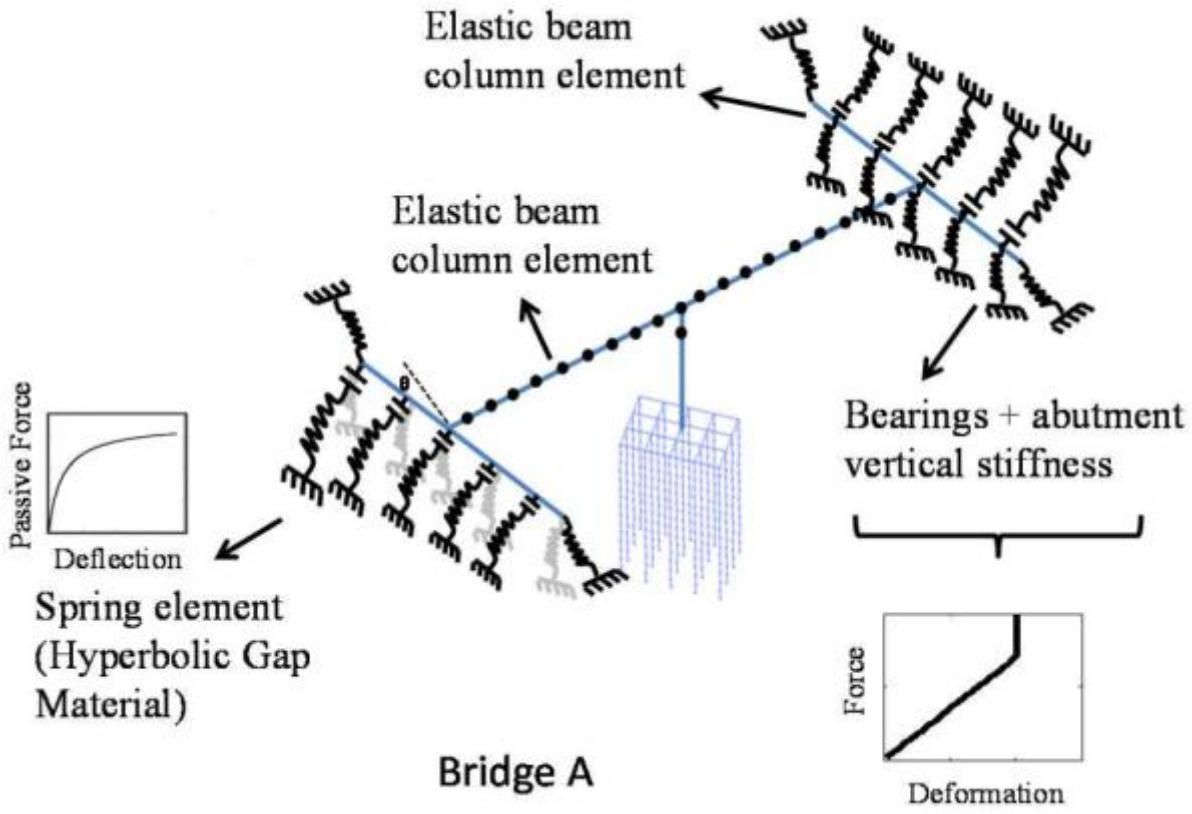

Figure 4: Stick Model of Bridge A Geometrical and material Properties (Mobasher 2016)

The concrete deck was considered to be elastic and have a concrete capacity f'_c and Elastic modulus E_c of 5 ksi and 4030.5 ksi, respectively. The concrete capacity of the column also has an f'_c of 5 ksi and the steel reinforcing is ASTM A706. A simplified abutment was considered in the OpenSees model and four elastomeric bearing pads were used per abutment (Mobasher 2016). The following table summarizes the geometrical and material properties of the bridge model.

Exterior shear keys were implemented at each abutment to mitigate the transverse displacement of the deck. The force-deformation of the shear key utilized herein is brittle. The angle of the inclined face of the shear key (β) is 67˚, the angle of kinking of the shear key (α) if 37˚, and the coefficient of friction (μ_r) is taken as 36% (Mobasher 2016). The yield strength of the bridge's shear key (f_y) is 68 ksi while the ultimate strength (f_u) is considered as 95 ksi. The shear key seat width is modeled in OpenSees to be 30 in., the height is 56 in. with a depth of 50 in. (Mobasher 2016).

Bridge Characteristic	Value
Year built	2001
Abutment Skew Angle	33˚
Number of spans	2
Lengths of Spans	Span 1 = 110.25 ft. Span 2 = 110.25 ft.
Deck type	Concrete cast-in-place
Total length of bridge	220.4 ft.
Bridge deck width	27.13 ft.
Bridge deck depth	4.64 ft.
Bridge Characteristic	**Value**
Cross-Sectional Area *(A)*	97.55 ft.^{2}
Cross-sectional Moment of Inertia *(I)*	I_x = 180.328 ft.^{4} I_y = 3797.9 ft.^{4}
Cross-sectional Shear Area *(A_v)*	A_{vx} = 18.92 ft.^{2} A_{vy} = 27.58 ft.^{2}
Cross-sectional Section Modulus *(Z)*	Z_x = 115.14 ft.^{3} Z_y = 521.83 ft.^{3}
Cross-sectional Plastic Modulus *(S)*	S_x = 83.35 ft.^{3} S_y = 279.97 ft.^{3}
Total column height	22 ft.
Clear height of column	19.68 ft.
Elastic deck superstructure concrete material properties	f'_c = 5 ksi E_c = 4030.5 ksi
Column bent concrete material properties	f'_c = 5 ksi ASTM A706 reinforcing steel
Column bent cross-section reinforcing detail	Longitudinal reinforcement = (44) #11 bars Transverse reinforcement = #6 @ 3.5” o.c. (spiral)
Abutment model	Simplified abutment
Abutment bearing pads	4 elastomeric bearing pads per abutment

Table 1: OpenSees computer generate bridge geometric and material properties

The columns of the bridge models incorporate a lumped plasticity, in which the plastic behavior of the bridge is relegated to hinges located at the ends of linear elastic zone. The elements of the bridge are modeled in OpenSees through the use of the `beamWithHinges`, which incorporates the modified Gauss-Radau integration rule (Scott and Fenves 2006). The plastic regions of the columns model the nonlinear steel fiber sections through the `ReinforcingSteel` command, while the nonlinear concrete fiber sections use the command, `concrete01`. This concrete material command assumes no tensile strength and accounts for the inherent unloading and reloading of the concrete’s stiffness in a linear manner. The model assumes a rigid elastic element for the section of the vertical column that is incorporated in the deck; the node of interest, Node 12, is defined to be a part of this rigid elastic element section. Both spans of the bridge’s deck are modeled by incorporating `elasticBeamColumn` for 10 elements; the lumped mass at each

node in the deck integrates the rotational and translational mass of the elements it encompasses (Mobasher 2016). The abutments of the bridge model considered herein assume rigid elements and are rigidly connected to the main structure of the bridge at its centerline. The geometric properties of the abutments assume dimensions of 16x2 in^2.

2.2 Validation of Bridge Model through Seismic Performance

The underlying logic behind the performance-based validity of the simulations considers the comparison between the behavior of the bridge when subjected to recorded Northridge ground motions to the behavior of the bridge due to the simulations produced for each ground motion station. The intensity measures of the records between the recorded and the simulated should ideally be similar; however, the true indicator of validity was taken to be the comparison between the maximum drift of the column when experiencing recorded versus simulated motion. If the behavior of the bridge is statistically similar whether it is experiencing recordings or simulations and the statistical distributions of the significant intensity measures, primarily the mean and variance, of the recorded and simulated data, then these artificially-produced ground motions may be used as meaningful supplements to performance-based design. The following section explores this method and provides conclusions derived from the results of measured intensity measures, recorded design parameters, and bridge performance.

CHAPTER 3: Analysis and Results

An analysis of six intensity measures, all of which are derived from ground motion time history accelerations, was performed in relation to their significance in predicting bridge performance and the difference in statistical distribution of the actual parameters between the recorded and simulated data. The IMs represent different characteristics of a particular ground motion record and are used as parameters to identify that data record. A linear regression of logged recorded intensity measures with respect to their prediction of the recorded EDP narrowed down the significant intensity measures, which attributed to accurate EDP estimations. This method was repeated on the simulated ground motions and corresponding EDP to evaluate comparisons between the recorded and simulated regression models. Ground motion station number, simulation realization number, and ground motion angle of attack were considered as potential random effects in affecting significance of estimating EDP. The following sections provide a detailed analysis of the methods employed throughout this research, the conclusions derived from the results of the analysis and suggestions for future research concerning simulated ground motion time history acceleration records and their practicalities.

3.1 Preliminary Considerations and Validation Methodology

3.1.1 Intensity Measures

The intensity measures originally considered are stated below; for full definitions of the intensity measures as used in this report, refer to Appendix A.2.

1. Normalized Arias Intensity (I_a)
2. Significant Duration (T_d)
3. Mid-duration (t_{mid})
4. Rate of Energy accumulation (I_a/T_d)
5. Slope of Predominant Frequency (ω')
6. Predominant Frequency at Mid-duration (ω_{mid})

Originally, ground motion records (recorded and simulated) were separated into their X and Y components and the intensity measures were calculated for each directional component (i.e. the Arias Intensity in the X direction would be depicted as I_{ax}). Techniques utilized in combining the components of the ground motion records through the intensity measures and the reason behind doing so are described subsequently.

3.1.2 Engineering Demand Parameter

As previously discussed, the performance of a two-span, single column bridge coded in OpenSees was used to validate the simulated ground motions. Node 12, as depicted in Figure 3, was taken as the point of interest. The displacement of Node 12 in the x and y direction was recorded and the square root of the sum of the squares (SRSS) of the x and y records was taken as the EDP of the bridge.

3.1.3 Direction of Ground Motions

Preliminary data was compiled using a single angle of rotation, equal to zero, for the ground motions records (for both recorded and simulated). Thus, the following Preliminary Results section consists of results based off ground motion records run at solely 90 degrees with respect to the bridge. The incorporation of ground motion angle of rotation is introduced later in the research.

3.1.4 Preliminary Bridge Results—Recorded Ground Motions

The six IMs described above were obtained for both the x and y directions and a linear regression was run to determine significant IMs for the recorded motions. The results below consider all six parameters and reflect the raw recorded values (no transformations were applied to the variables). The figures presented below show the output of Rstudio, which was used to run all regressions referenced in this research. All units are Imperial.

```
lm(formula = EDPRec ~ IaxRec + DurxRec + TmidxRec + ADxRec +
    WprimexRec + WmidxRec, data = REC)

Residuals:
    Min      1Q  Median      3Q     Max
-1.7771 -0.3399 -0.1037  0.2026  4.4942

Coefficients:
             Estimate Std. Error t value Pr(>|t|)
(Intercept)  3.5403338  1.3895932   2.548   0.0160 *
IaxRec      -0.0005952  0.0105533  -0.056   0.9554
DurxRec     -0.1041802  0.0705062  -1.478   0.1496
TmidxRec     0.0340902  0.0877573   0.388   0.7003
ADxRec       0.1310546  0.0661452   1.981   0.0565 .
WprimexRec   3.0346151  3.6560707   0.830   0.4129
WmidxRec    -0.3793626  0.2037660  -1.862   0.0721 .
---
Signif. codes:  0 '***' 0.001 '**' 0.01 '*' 0.05 '.' 0.1 ' ' 1

Residual standard error: 1.029 on 31 degrees of freedom
Multiple R-squared:  0.8162,    Adjusted R-squared:  0.7806
F-statistic: 22.95 on 6 and 31 DF,  p-value: 3.906e-10
```

Figure 5.a: Recorded X-Direction linear regression results

```
lm(formula = EDPRec ~ IayRec + DuryRec + TmidyRec + ADyRec +
    WprimeyRec + WmidyRec, data = REC)

Residuals:
    Min      1Q  Median      3Q     Max
-1.6896 -0.4694 -0.1992  0.2749  4.3466

Coefficients:
             Estimate Std. Error t value Pr(>|t|)
(Intercept)  3.58793    1.38501   2.591   0.0145 *
IayRec       0.03125    0.01729   1.808   0.0804 .
DuryRec     -0.06314    0.06529  -0.967   0.3410
TmidyRec    -0.03360    0.09185  -0.366   0.7170
ADyRec      -0.07145    0.09706  -0.736   0.4672
WprimeyRec   1.01818    3.26109   0.312   0.7570
WmidyRec    -0.36115    0.18986  -1.902   0.0665 .
---
Signif. codes:  0 '***' 0.001 '**' 0.01 '*' 0.05 '.' 0.1 ' ' 1

Residual standard error: 1.185 on 31 degrees of freedom
Multiple R-squared:  0.7562,    Adjusted R-squared:  0.709
F-statistic: 16.02 on 6 and 31 DF,  p-value: 2.711e-08
```

Figure 5.b: Recorded Y-Direction linear regression results

Given a constraining p-value of 0.05, the results above show no significance to any parameters; furthermore, it is clearly indicated that the bias plays a larger role in determining the EDP of node 12 than the actual IMs. I_a/T_d (which is the Arias Intensity divided by the Significant Duration and represents the rate of energy accumulation), is obviously highly correlated to the parameters Arias Intensity and Duration. Intensity measure, I_a/T_d, was removed from the linear regression, since the regression does not convey accurate results with highly-correlated parameters; the results from the regression sans I_a/T_d are shown in Table 2 and indicate an improvement from the previous results obtained in Figure 5.

IM	**Slope Estimate**	**P-Value**	**Significance Level**	**R squared**	**Residual Error**
Intercept	3.82	0.01	*	0.79	1.08
I_{ax}	-0.02	8.57e-07	***		
T_{dx}	-0.14	0.06	.		
T_{midx}	0.07	0.44			
ω'_x	4.72	0.21			
ω_{midx}	-0.42	0.06	.		

Table 2: Linear Regression for recorded X-direction components with 5 IMs

Similar results to those shown in Table 2 were obtained for the linear regression with 5 IMs in the y direction and are available in Appendix A.3.1. This preliminary regression provided enlightenment on the level of significance and influence each parameter possessed in predicting the drift of Node 12. Given the results of the linear regression for the 5 IMs, the parameters used in the subsequent regressions were the significant parameters of Arias Intensity, Significant Duration, and ω_{mid}. The results of the linear regression in the X-direction using the three significant intensity measures are shown below in Table 3. Results pertaining to Y-directional ground motions are similar and provided in Appendix A.3.2.

IM	**Slope Estimate**	**P-Value**	**Significance Level**	**R squared**	**Residual Error**
Intercept	3.79	0.01	*	0.78	1.08
I_{ax}	0.02	2.16e-07	***		
T_{dx}	-0.10	0.02	*		
ω_{midx}	-0.43	0.05	*		

Table 3: Linear Regression for recorded X-direction components with 3 significant IMs

As seen through the disparities in the p-value of the intensity measures between Table 2 and Table 3, illuminating insignificant parameters provides more significance and value on the parameters which influence the EDP of the bridge. The coefficients of the significant IMs remained relatively unchanged; however, the meaningfulness the intensity measures provided towards estimating the drift of Node 1 increased. Given the results above, it's concluded that these three parameters (Arias Intensity, Significant Duration, and predominant frequency at mid duration) are significant in estimating the bridge's EDP and follow the linear regression equation shown below. The equation provided below is for the X-direction ground motions; since the coefficients for the Y-direction were similar and the significant intensity measures were identical, the linear regression equation for the Y-directional ground motions is omitted in an effort to reduce redundancy.

$$EDP^{rec} = 3.788 + 0.02I_{ax}^{rec} - 0.102T_{dx}^{rec} - 0.434w_{midx}^{rec} + \varepsilon$$

The residuals of the linear regression with three significant parameters were plotted to ensure that the residuals did not follow a certain trend and that the linear regression was viable. The residuals are plotted below and incorporate both orthogonal directions.

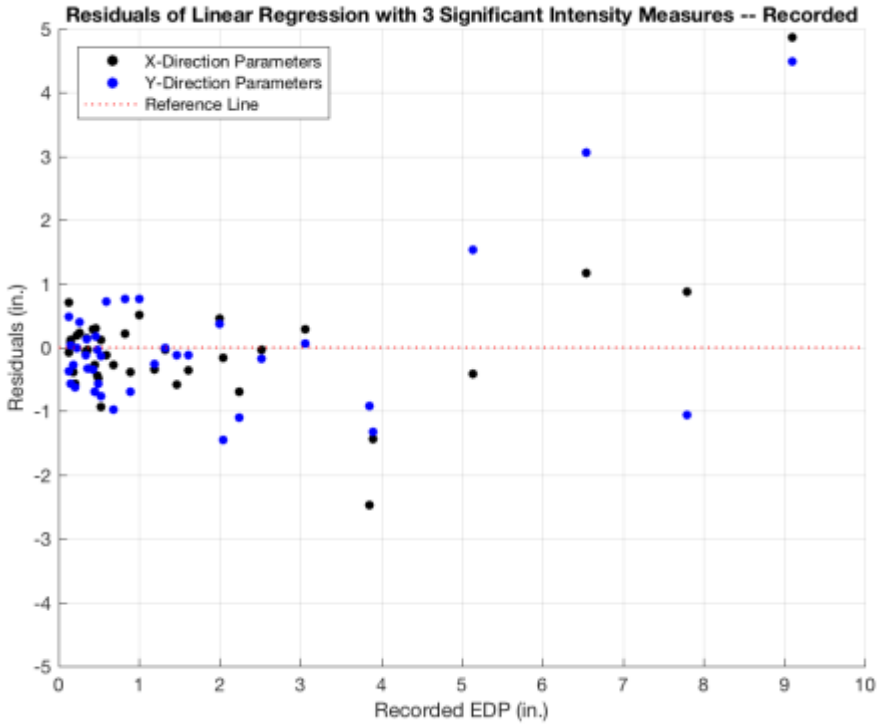

Figure 6: Raw recorded residuals from 3-parameter linear regression

There is clearly a problematic trend in the residuals displayed in Figure 6. The evaluated Node 12 is 264 inches in elevation height; thus the column should being to experience plastic behavior around 4 inch displacement at the top. Figure 6 captures this transformation around 3 to 4 inches, a point at which the linear regression is incapable of accurately estimating the EDP due to recorded ground motions. Beyond the 4 inch mark on the graph above, there is a trend in the residuals; as the EDP increases, the inaccuracy in the regression increases. It was concluded that a linear regression of raw intensity measures was unable to provide meaningful results. Consequently, a transformation of the parameters was deemed necessary. Three transformations were considered:

1. Logarithmic Transformation
2. Reciprocal Transformation
3. Square Root Transformation

The logarithmic transformation proved to yield the most meaningful results and provided acceptable residuals for the recorded linear regression. EDPs were assumed to follow a lognormal distribution. The results from this logarithmic transformation are presented in the following section.

3.2 Evolution of Validation Methodology

3.2.1 Linear Regression of Logged Variables:

A linear regression of the logged variables considering all six IMs was first employed; the results are presented in Appendix A.3.3. Similar to the regression results of the raw recorded parameters, the significant intensity measures were Arias Intensity, Significant Duration, and ω_{mid}. Displayed below are the linear regression results from the logged data in the X-direction accounting for the three significant IMs. The corresponding regression formula for the X-direction ground motions accompanies the table. Linear regression results of the logged data in the Y-direction are presented in Appendix A.3.4a.

IM	Slope Estimate	P-Value	Significance Level	R squared	Residual Error
Intercept	1.02	0.25		0.94	0.31
$Ln(I_{ax})$	0.59	3.61e-12	***		
$Ln(T_{dx})$	-0.67	0.002	**		
$Ln(\omega_{midx})$	-0.89	0.001	***		

Table 4: Linear Regression of recorded logged parameters in the X-Direction

$$Ln(EDP^{rec}) = 1.02 + 0.59Ln(I_{ax}^{rec}) - 0.666Ln(T_{dx}^{rec}) - 0.889Ln(w_{midx}^{rec}) + \varepsilon$$

The residuals of the linear regression performed with log-transformed recorded ground motion parameters are depicted below. Figure 7 displays the regression residuals for X-directional ground motions in black and for Y-directional ground motions in blue. The dotted red lines are provided for reference as the residuals should ideally hover close to the X-axis.

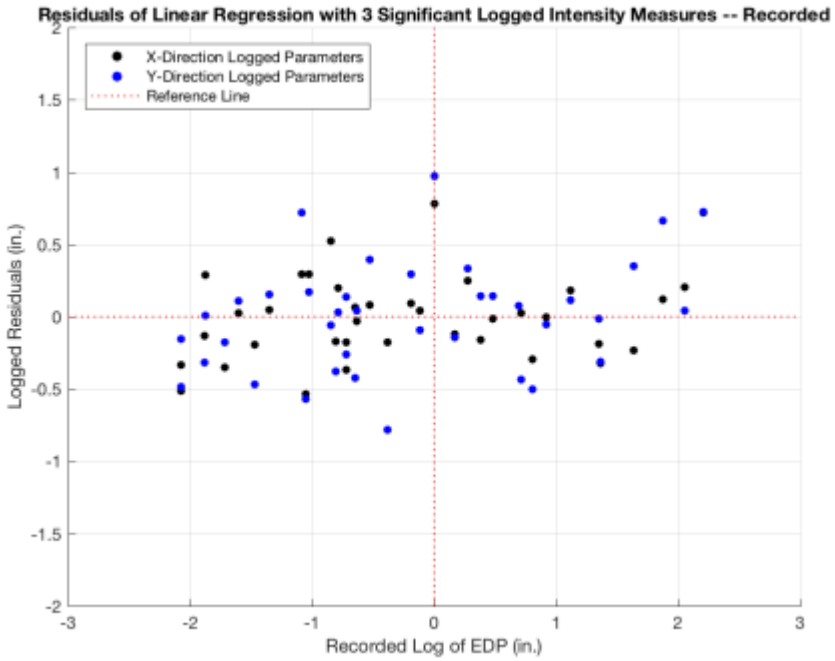

Figure 7: Residuals of Logged Linear Regression for Recorded Ia, T_d, and ω_{mid}

3.2.2 Preliminary Mixed Effects Regression on Simulations

As discussed in the previous section, the appropriate model for the recorded ground motions considered three significant parameters (Arias Intensity, Significant Duration, and ω_{mid}) in the logarithmic domain. Since the purpose of the simulations is to replicate the effect the recorded parameters has on the EDP of the bridge, a regression of logged simulated variables using the three IMs found to be significant in the recorded set was performed. Preliminary data from the simulations considered twenty realizations for each type of simulation methodology (GMSV_17_3/NR 2017).

A mixed effects regression of the model was performed on the logged intensity measures and EDP to consider the effect the simulation run had on the ability of the intensity measures to estimate the bridge's EDP. For all simulation methodologies, EXSIM, GP, IRIK, SDSU, and SONG, simulation run did not influence the fixed intercepts. For this reason, subsequent results only used one simulation realization from each of the simulation methodologies, given that the run did not have an effect on the regression. Results are displayed and articulated further in Section 4.7, in which a complete mixed effects regression. The completed mixed effects regression considered mixed effects from ground motion station, simulation run, and ground motion angle of rotation.

3.3 Significant Intensity Measures

The logarithmic model discussed above was deemed meaningful and appropriate due to multiple reaffirming factors. When extracting the unnecessary IMs from the 6-parameter regression, the previously significant IMs increase in significance. Moreover, the intercept, or the bias, is no longer significant; this indicates that the intercept need not be in the linear regression equation and provides no significance in estimating the EDP. This formulation was adopted for all regression equations with no significant bias. Thus, the regression equation could very well be the following:

$$Ln(EDP^{rec}) = 0.59Ln(I_{ax}^{rec}) - 0.67Ln(T_{dx}^{rec}) - 0.89Ln(w_{midx}^{rec}) + \varepsilon$$

Furthermore, 94% of the variance from the model can be accounted for by these three Intensity Measures. Given these meaningful results, subsequent data and results refer to IMs and EDP solely in the logarithmic domain.

Regression results were obtained for the five different simulation methodologies (EXSIM, GP, IRIK, SDSU, and SONG) using the significant IMs from the recorded regression outcomes. A linear regression was performed for each simulation methodology using the log of the Arias Intensity, Significant Duration, and ω_{mid} as the independent variables estimating the log of the EDP. The following sections display the regression equations and their corresponding residuals for each simulation methodology. The results presented below represent the X-directional ground motion component. Results from the Y-directional component were similar to the ones presented below and are thus referenced in Appendix A.3.4.b to avoid redundancy.

3.3.1 EXIM Linear Regression with Logarithmic Parameters

IM	Slope Estimate	P-Value	Significance Level	R squared	Residual Error
Intercept	-1.37	<2e-16	***	0.93	0.21
$Ln(I_{ax})$	0.601	<2e-16	***		
$Ln(T_{dx})$	-0.18	2.17e-05	***		
$Ln(\omega_{midx})$	-0.20	5.84e-06	***		

Table 5: Linear Regression of EXSIM logged parameters in the X-Direction

$$Ln\left(EDP^{exsim}\right) = -1.37 + 0.601Ln\left(I_{ax}^{exsim}\right) - 0.18Ln\left(T_{dx}^{exsim}\right) - 0.20Ln\left(w_{midx}^{exsim}\right) + \varepsilon$$

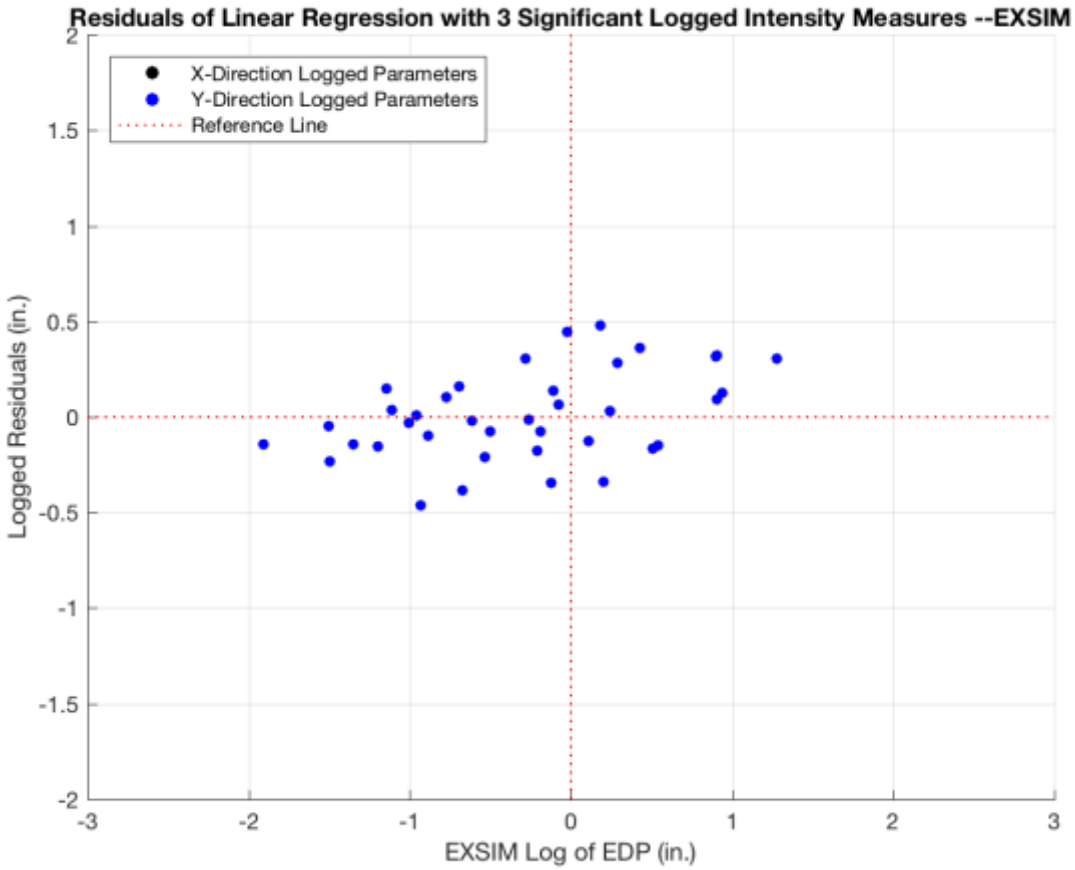

Figure 8: Residuals of Linear Regression for EXSIM Ln(Ia), Ln(T_d), and Ln(ω_{mid})

Figure 8 portrays the regression results for the logged EXSIM parameters of Arias Intensity, Significant Duration, and predominant frequency at mid duration for both orthogonal components. Only one simulation realization is used due to the fact that the preliminary mixed effects regression found simulation realization to be provide no effect on the intercept estimates. Ground motion records for the EXSIM simulation methodology have identical x and y directional

time history acceleration; only one color appears on the graph in Figure 8 because the residuals in the x and y direction are identical.

3.3.2 GP Linear Regression with Logarithmic Parameters

IM	Slope Estimate	P-Value	Significance Level	R squared	Residual Error
Intercept	-0.18	0.17		0.92	0.24
$Ln(I_{ax})$	0.63	<2e-16	***		
$Ln(T_{dx})$	-0.44	<2e-16	***		
$Ln(\omega_{midx})$	-0.5	<2e-16	***		

Table 6: Linear Regression of GP logged parameters in the X-Direction

$$Ln(EDP^{gp}) = 0.63Ln\left(I_{ax}^{gp}\right) - 0.44Ln\left(T_{dx}^{gp}\right) - 0.5Ln\left(w_{midx}^{gp}\right) + \varepsilon$$

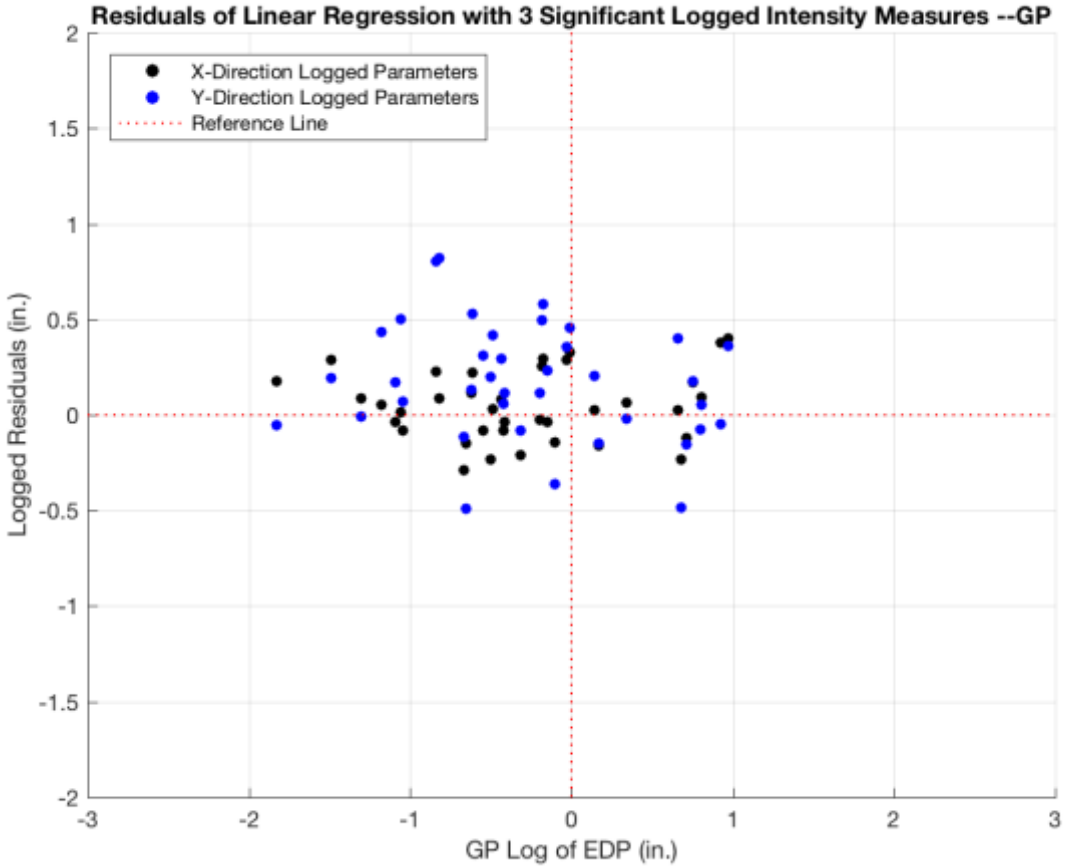

Figure 9: Residuals of Linear Regression for GP Ln(Ia), Ln(T_d), and Ln(ω_{mid})

A linear regression of on realization of the GP simulation methodology using logarithmic IMs Arias Intensity, Significant Duration, and ω_{mid} was capable of accurately estimating the EDP of the bridge due to the simulation motion.

Table 6 shows that the bias in the regression holds no significance in estimating the EDP and may be omitted from the regression equation. All three IMs that were significant in the recorded regression are also extremely significant in the GP regression.

Furthermore, Figure 9 shows that there is no, if not slight, trend in the residuals of the regression. Positive residuals indicate that the regression is underestimating the given EDP, while negative residuals signify that the regression is overestimating the drift of Node 12 due to the GP time-history. The residuals due to X-directional ground motion components tend to hover around the reference lines, while the Y-directional components tend more to be underestimated by the regression. Despite this difference between the orthogonal components, the three IMs contrived from the GP simulation methodology do not underestimate or overestimate the bridge's EDP by more than 2inches or 0.6 inches, respectively. The GP model explains almost 92% of the variability in the EDP due to GP ground motions around its mean.

3.3.3 IRIK Linear Regression with Logarithmic Parameters

IM	Slope Estimate	P-Value	Significance Level	R squared	Residual Error
Intercept	-0.21	0.08	.	0.91	0.24
Ln(I_{ax})	0.63	<2e-16	***		
Ln(T_{dx})	-0.39	<2e-16	***		
Ln(ω_{midx})	-0.53	<2e-16	***		

Table 7: Linear Regression of IRIK logged parameters in the X-Direction

$$Ln\left(EDP^{irik}\right) = 0.63Ln\left(I_{ax}^{irik}\right) - 0.39Ln\left(T_{dx}^{irik}\right) - 0.53Ln\left(w_{midx}^{irik}\right) + \varepsilon$$

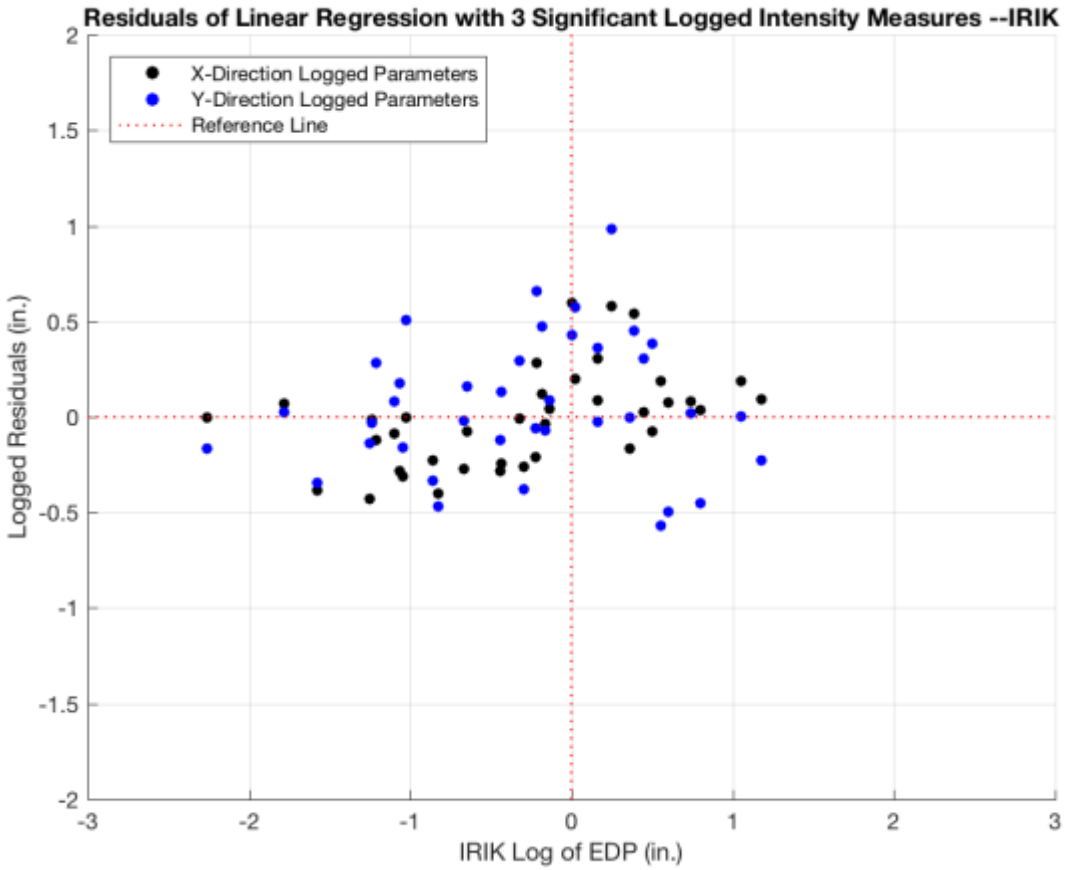

Figure 10: Residuals of Linear Regression for IRIK Ln(Ia), Ln(T_d), and Ln(ω_{mid})

The regression intercept for the IRIK simulation methodology was not significant in estimating the IRIK simulated EDP and thus, was not included in the above regression equation. The three IMs that were significant in the recorded regression are also incredibly significant in the IRIK simulated regression. 90% of the variability in the IRIK acquired EDP of the bridge is accounted for by these three intensity measures. Furthermore, the residuals of the IRIK regression show no significant trend and both orthogonal components area capable of estimating the EDP due to IRIK simulated ground motions with suitable accuracy. In comparing this model to the recorded ground motion regression model, the IRIK simulation methodology, similar to the GP methodology, provide similar trends and significance.

3.3.4 SDSU Linear Regression with Logarithmic Parameters

IM	Slope Estimate	P-Value	Significance Level	R squared	Residual Error
Intercept	-0.27	0.15		0.88	0.35
$Ln(I_{ax})$	0.54	<2e-16	***		
$Ln(T_{dx})$	-0.42	<2e-16	***		
$Ln(\omega_{midx})$	-0.29	0.01	**		

Table 8: Linear Regression of SDSU logged parameters in the X-Direction

$$Ln(EDP^{sdsu}) = 0.54Ln(I_{ax}^{sdsu}) - 0.43Ln(T_{dx}^{sdsu}) - 0.29Ln(w_{midx}^{sdsu}) + \varepsilon$$

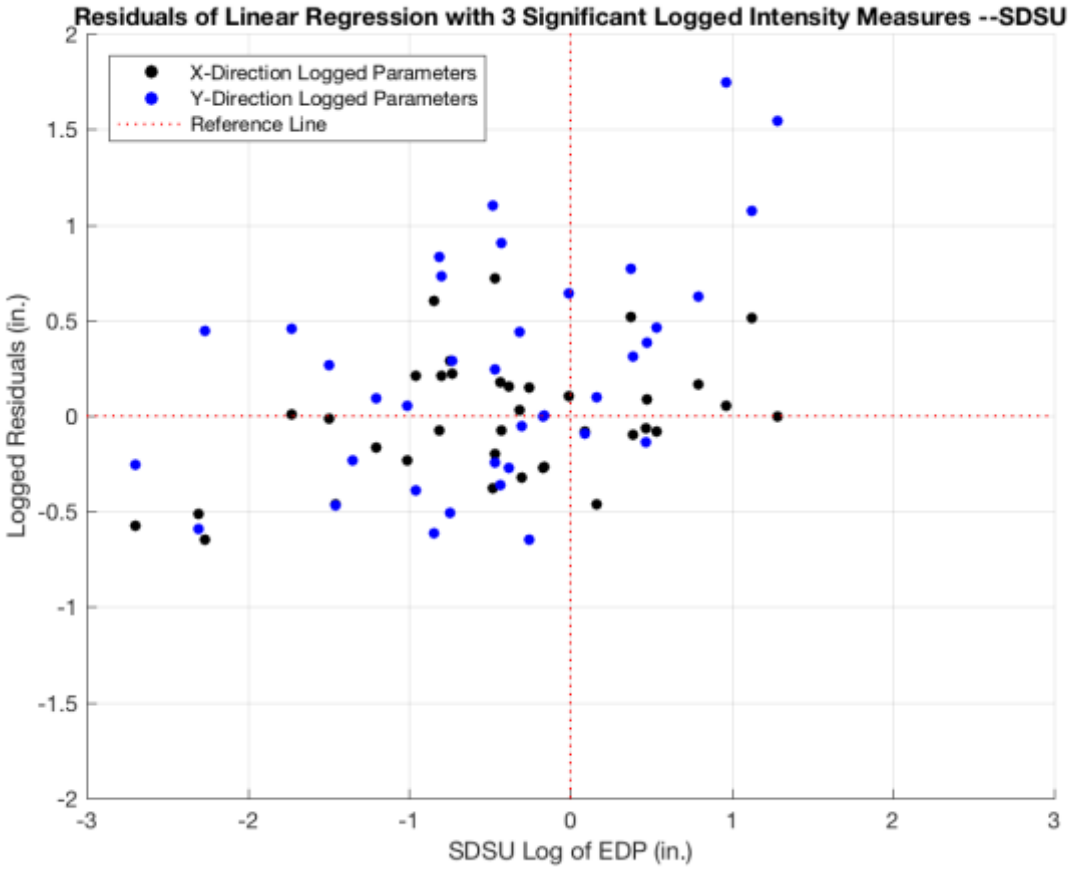

Figure 11: Residuals of Linear Regression for SDSU Ln(Ia), Ln(T_d), and Ln(ω_{mid})

Although a linear regression of SDSU logarithmic parameters provided no significant bias and proper significant intensity measures, the residuals of the regression present a problematic trend in the graph depicted above. Particularly troublesome is the Y-directional component, in which there is an obvious upward trend; as the drift of Node 12 due to SDSU simulated ground motions increases, the linear regression is incapable of accurately estimating the EDP and in fact increasingly underestimates it. Furthermore, the residuals obtained from the SDSU regression pose much larger inaccuracies than that of EXSIM, GP, or IRIK. SDSU was unable to capture the same amount of variation in its corresponding EDP due to the three significant intensity measures

as well as the other simulation methodologies. Additional factors clearly affect the accuracy of EDP estimation. Based off the results presented above, further research and tailoring of SDSU-methodology time history records is recommended.

3.3.5 SONG Linear Regression with Logarithmic Parameters

IM	Slope Estimate	P-Value	Significance Level	R squared	Residual Error
Intercept	-0.15	0.16		0.92	0.26
$Ln(I_{ax})$	0.64	<2e-16	***		
$Ln(T_{dx})$	-0.58	<2e-16	***		
$Ln(\omega_{midx})$	-0.31	5.01e-10	***		

Table 9: Linear Regression results of SONG logged parameters in the X-Direction

$$Ln(EDP^{song}) = 0.64Ln\left(I_{ax}^{song}\right) - 0.58Ln\left(T_{dx}^{song}\right) - 0.31Ln\left(w_{midx}^{song}\right) + \varepsilon$$

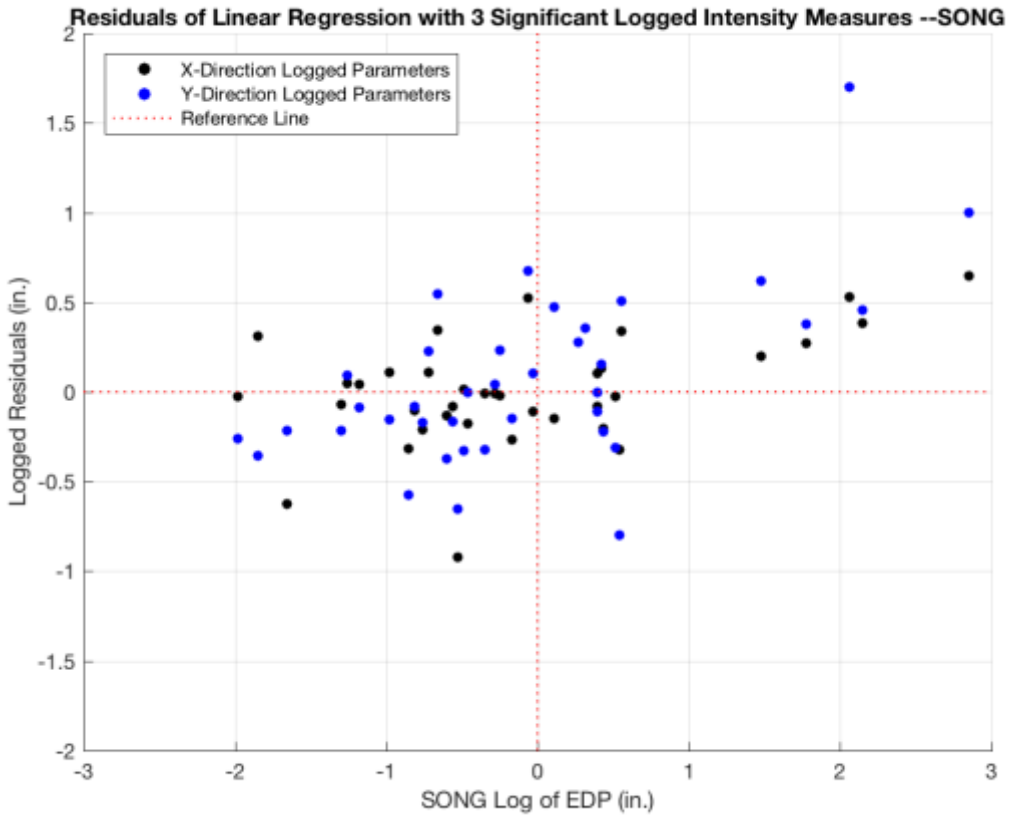

Figure 12: Residuals of Linear Regression for SONG Ln(Ia), Ln(T_d), and Ln(ω_{mid})

The SONG simulation methodology performed similar to that of SDSU in the linear regression of the logged parameters. The bias had no significance, the three intensity measures that were significant with the recorded data were also very significant in with SDSU, and 91% of the variability around the estimation of EDP could be explained through these three IMs. Despite such positive results, the graph of the residuals shows an incredible trend in that the linear

regression consistently underestimates the drift of Node 12 due to SONG ground motions and increasingly does so as the drift increases. Based off the results presented above, further research and tailoring of SONG-methodology time history records is recommended.

The slight to no trend seen in the residuals of EXSIM, GP, and IRIK is not particularly alarming given that the parameters used in the linear regression were IMs that were significant in the recorded linear regression, regardless of those significant in the corresponding simulated regression. Across all simulation methodologies, Arias Intensity and Significant Duration were significant. However, the other parameters (ω', ω_{mid}, and T_{mid}) varied in significance in a linear regression using all six IMs; for the most part, significance varied between ω' and ω_{mid}. Choosing IMs that were significant in the recorded data set and using those parameters to perform a regression on the simulation methodologies allowed for a comparison between how closely the simulations follow the recordings in terms of their value and their effect on the bridge's EDP.

3.4 Standard Normal Domain Transformations

Because the different intensity measures inherently possess different distributions, all parameters were transformed into the standard normal domain according to their respective characterizing distributions. The intensity measures and their distributions are shown below. Transformations into the standard normal domain were applied according to methodology discussed in PEER Report 2010/02 (Rezaeian and Der Kiureghian 2010).

1. Ln(I_a)—Standard Normal Distribution
2. T_d—Beta Distribution
3. T_{mid}—Beta Distribution
4. ω_{mid}—Gamma Distribution
5. ω'—Two-sided Truncated Exponential Distribution

The following table displays the results from the linear regression with un-transformed and transformed intensity measures in the X direction for the recorded ground motions. T_{mid} was not considered in the analysis since it failed to produce meaningful results. Label "NRT" denotes no Rezaeian transformations (the intensity measures are in the log domain); label "RT" denotes Rezaeian transformations as depicted in the list above. The results were similar in the y direction and are included in Appendix B.

IM	**Slope Estimate**		**P-Value**		**Significance Level**		**R squared**	
	NRT	RT	NRT	RT	NRT	RT	NRT	RT
Intercept	0.76	-2.78e01	0.45	1.57e-5		***	0.94	0.79
$Ln(I_{ax})$	0.63	4.8e-3	9.42e-13	1.14e-5	***	***		
$Ln(T_{dx})$	-0.62	-4.9e-01	0.006	0.1715	**			
$Ln(\omega_{midx})$	-0.78	-1.10	0.005	0.02	**	*		
$Ln(\omega'_x)$	0.06	-.05	0.37	0.11				

Table 10: Linear Regression resulst: Rezaeian transformed vs. Logged IMs

When transforming the intensity measures into the standard normal domain, the results from the linear regression showed that the Arias Intensity became much less significant in attributing to the estimation of the bridge's EDP. The bias, which was insignificant with the logged untransformed intensity measures, became significant in the standard normal domain. Furthermore, the percentage of the data accounted for by the variables (the value of R) decreased considerably from 94% to 78%.

Due to the factors mentioned above, it was decided to forgo transforming the variables into the standard normal space. Moving forward, analysis results were accomplished using the log of the intensity measures; the succeeding section describes the means in which the results deriving from the two orthogonal components of the ground motion were combined to provide more meaningful results when compared to the EDP.

3.5 Combining Orthogonal Components of Significant IMs

Upon transformation of the variables, a method to combine the orthogonal components of the IMs was developed. Because the EDP provides information on the behavior of the bridge from both the x and y directions, it is only appropriate to provide characterizations of combined orthogonal components of the IMs. Various characterizations of this combination were proposed; ultimately, the Arias Intensity was chosen to be reflected as the sum of square roots of its orthogonal components while T_d, ω_{mid}, and ω' were combined as geometric means. A full mathematical representation of these parameters is displayed below.

$$I_a = \sqrt{I_{ax}^2 + I_{ay}^2}$$

$$T_d = \sqrt{T_{dx} T_{dy}}$$

$$\omega_{mid} = \sqrt{\omega_{midx} \omega_{midy}}$$

$$\omega' = \sqrt{\omega'_x \omega'_y}$$

The following table shows results from a linear regression of the log of the significant recorded parameters when combining orthogonal components of the ground motions as described above.

IM	Slope Estimate	P-Value	Significance Level	R squared	Residual Error
Intercept	0.99	0.26		0.94	0.32
Ln(I_a)	0.58	1.62e-12	***		
Ln(T_d)	-0.69	0.001	**		
Ln(ω_{mid})	-0.92	0.001	***		

Table 11: Linear Regression of Recorded logged IMs with combined components

The R-squared values of the recorded regression increased significantly when combining the components through the methodology presented above. In comparison, simulated average R-squared value across all simulations rose from 0.89 to 0.92. The intercept remained insignificant in estimating the bridge's EDP through the linear regression and the three significant intensity measures remained Arias Intensity, Significant Duration, and ω_{mid}. The regression results remained very similar to the ones provided with using separate orthogonal components and thus, combining the orthogonal components of the ground motions to produce the combined intensity measures described above was deemed appropriate and meaningful.

To compare the intensity measures and the EDP of the simulations to the recorded data set, the recorded parameters (independent and dependent) were graphed against their simulated counterparts. The intensity measures considered were the ones which proved to be significant in the recorded data, (Arias Intensity, Significant Duration, and ω_{mid}) while the EDP considered was the maximum absolute drift of Node 12. The graphs on the following pages use data from one recorded set and one simulation realizations for each simulation methodology. The x and y components have been combined through the methodology previously mentioned above. The red dotted line is for reference of what a perfect 1:1 fitting should align with and the red trend line is the linear best fit line of the data displayed.

3.5.1 Arias Intensity

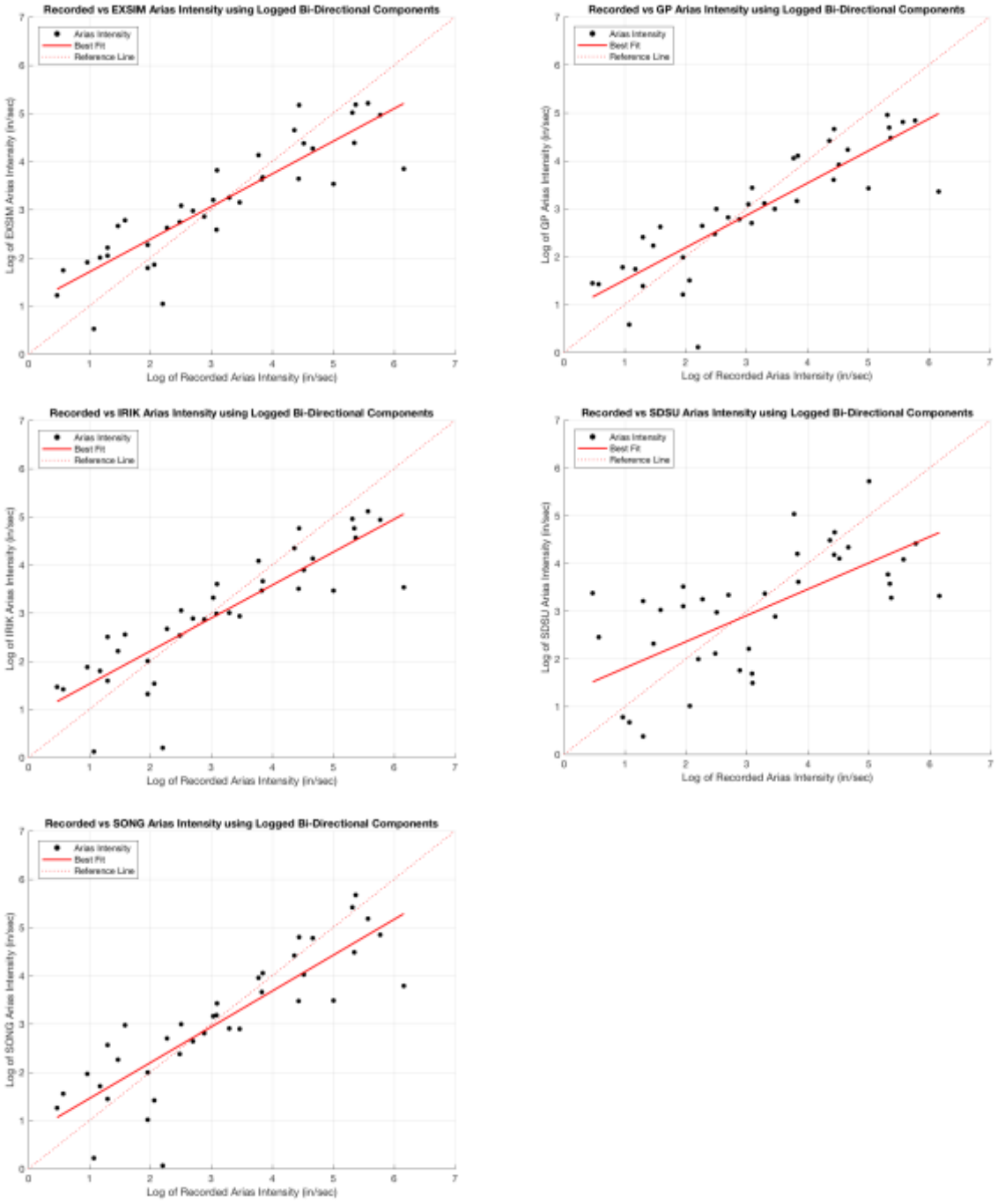

Figure 13: Recorded vs Simulated for Arias Intensity

Most of the simulation methodologies performed relatively similar to each other. As shown above, SDSU had the most variation in its Arias Intensity; however, on average, it's best fit line more closely aligns to the ideal 1:1 than the other simulations. For all simulations, if the Arias Intensity was below a threshold value of about 20 in/sec, the simulations overestimated their respective recorded ground motion energy. As the Arias Intensity increases, all simulations begin to underestimate their respective recorded Arias Intensity.

3.5.2 Significant Duration

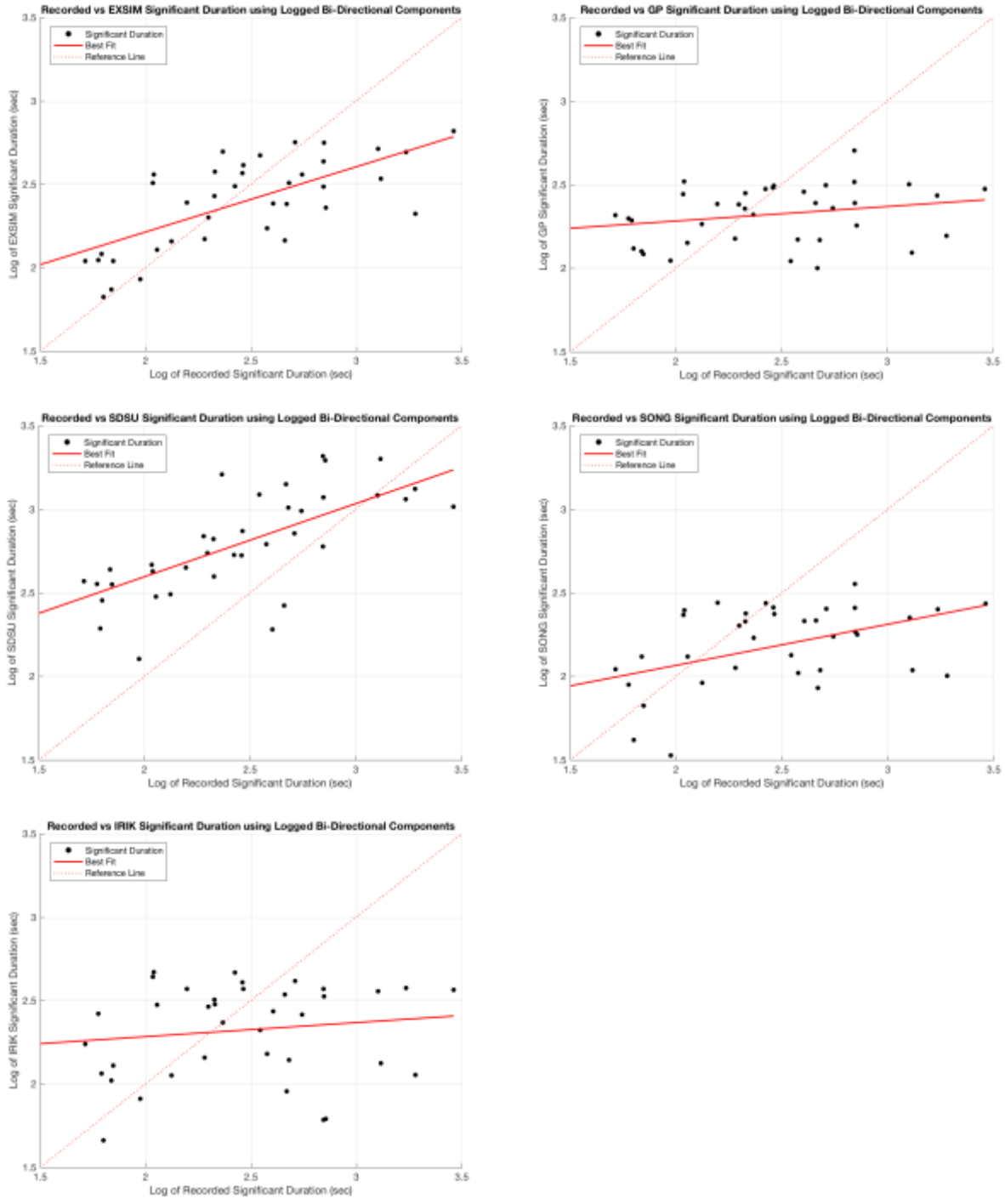

Figure 14: Recorded vs Simulated for Significant Duration

Simulated Significant Duration is relatively similar across all simulation methodologies. As recorded Duration increases, it's simulated counterparts tend to stay in the same range. There is a trend to be seen in EXSIM and SDSU; EXSIM Duration overestimated at lower durations and underestimated at higher durations while SDSU Duration overestimated recorded duration

across most realizations. As a significant intensity measure, Significant Duration is an area to consider for improvement in future realizations.

3.5.3 Predominant Frequency at Mid-Duration

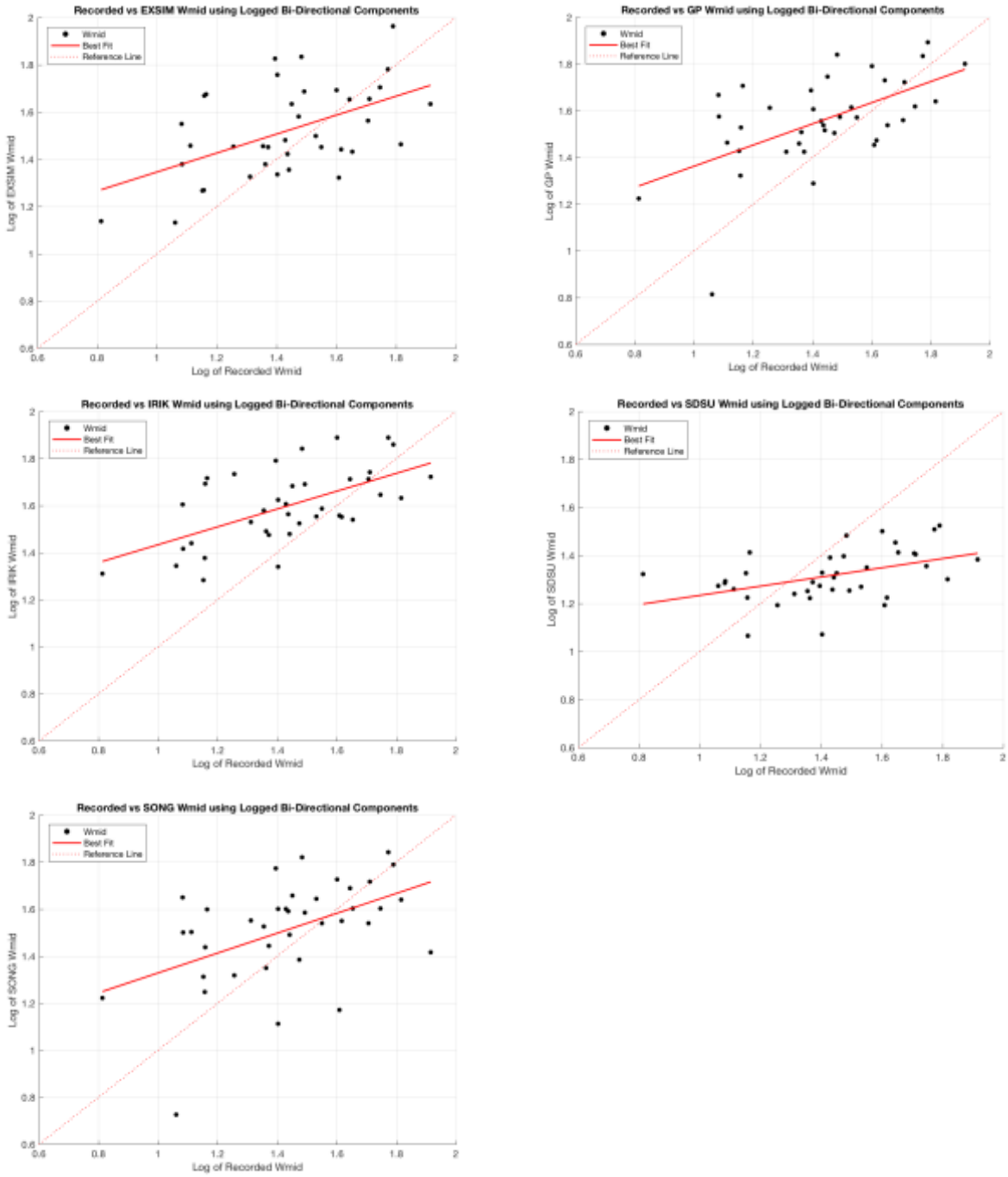

Figure 15: Recorded vs Simulated for ω_{mid}

For the significant intensity measure, ω_{mid}, the simulations increase with the predominant frequency at mid duration as the recorded increase. There is a trend seen here similar to the one seen with Arias Intensity where the simulations overestimate with respect to the recorded ω_{mid}

until they reach a threshold value (in this case about 4.48) and then subsequently underestimate ω_{mid} according to their recorded counterparts. SDSU does not have as prominent of a trend as the other simulations.

3.5.4 Engineering Demand Parameter

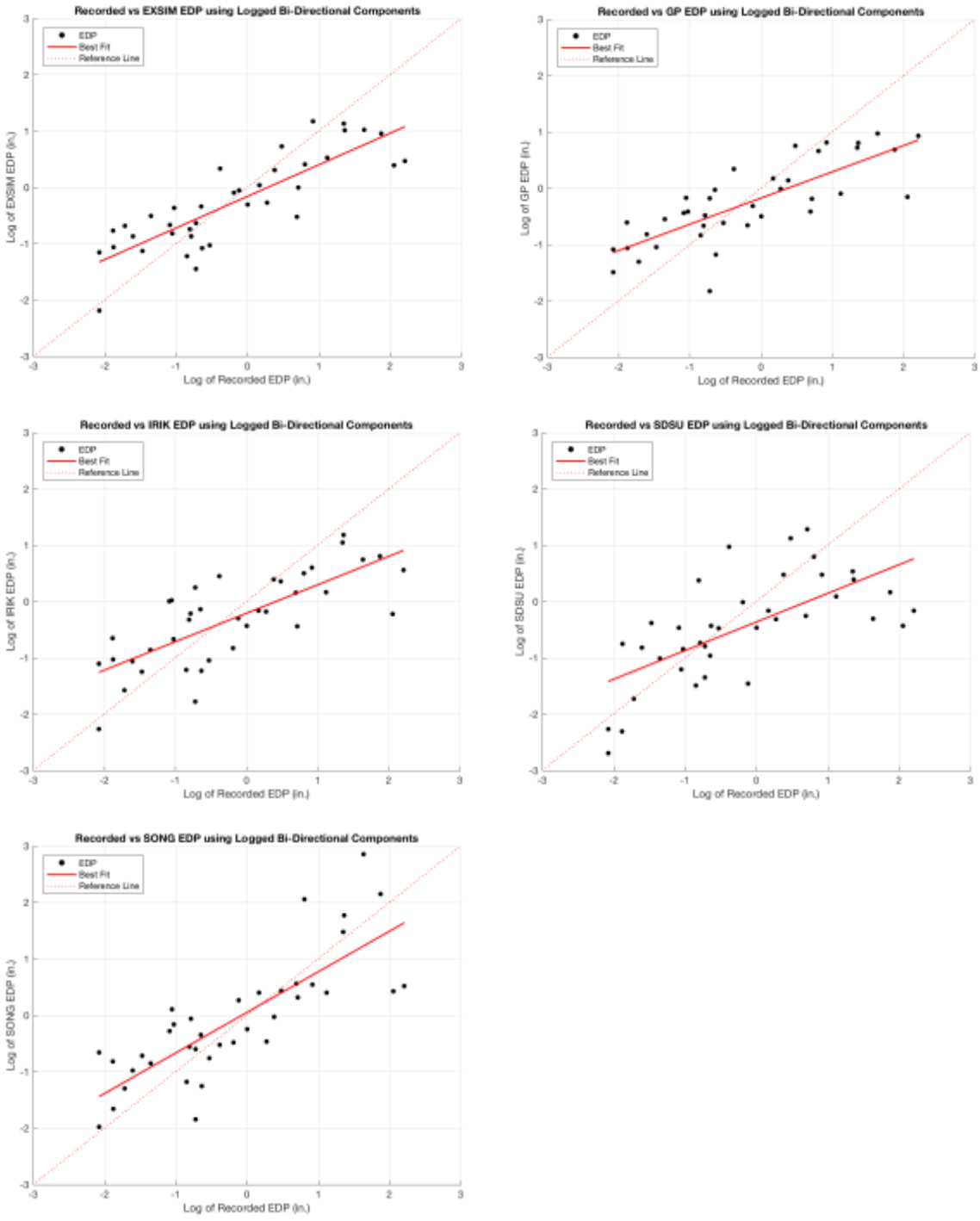

Figure 16: Recorded vs Simulated for EDP

The bridge's column maximum SRSS drift is plotted above; similar trends to the intensity measures are revealed in the column's behavior. The simulated EDP underestimates with respect to the recorded until about 1 inch of drift has occurred and then the simulated EDP start to overestimate with respect to the recorded EDP. There is a consistency here that is expected, that an increase in energy input would result in an increase of response. The expected consistency implies the connection and the estimating power of the significant intensity measures in relation to the maximum drift of Column Node 12.

3.6 Ground Motion Angle of Rotation

Previously, data was constructed based off a ground motion angle of 0 degrees with respect to the bridge's axis. The angle at which the ground motion is applied to the bridge was considered to investigate its effect on the IMs, the bridge's EDP, and the relationship between the two. Ground motions were rotated from 0 to 180 at 9 degree increments. A linear regression was applied to the log of recorded ground motion data set for all angles to evaluate the significant intensity measures when considering angle of rotation. The following table displays the results from this regression and the graph below shows the residuals produced from the regression. The regression results using the significant IMs found below for the simulated data is in Appendix A.3.5.

IM	Slope Estimate	P-Value	Significance Level	R squared	Residual Error
Intercept	0.94	7.99e-05	***	0.93	0.31
$Ln(I_a)$	0.58	<2e-16	***		
$Ln(T_d)$	-0.79	<2e-16	***		
$Ln(\omega')$	0.12	0.03	*		
$Ln(\omega_{mid})$	-0.88	<2e-16	***		

Table 12: Linear Regression of logged recorded parameters considering angles 0˚ to 180˚

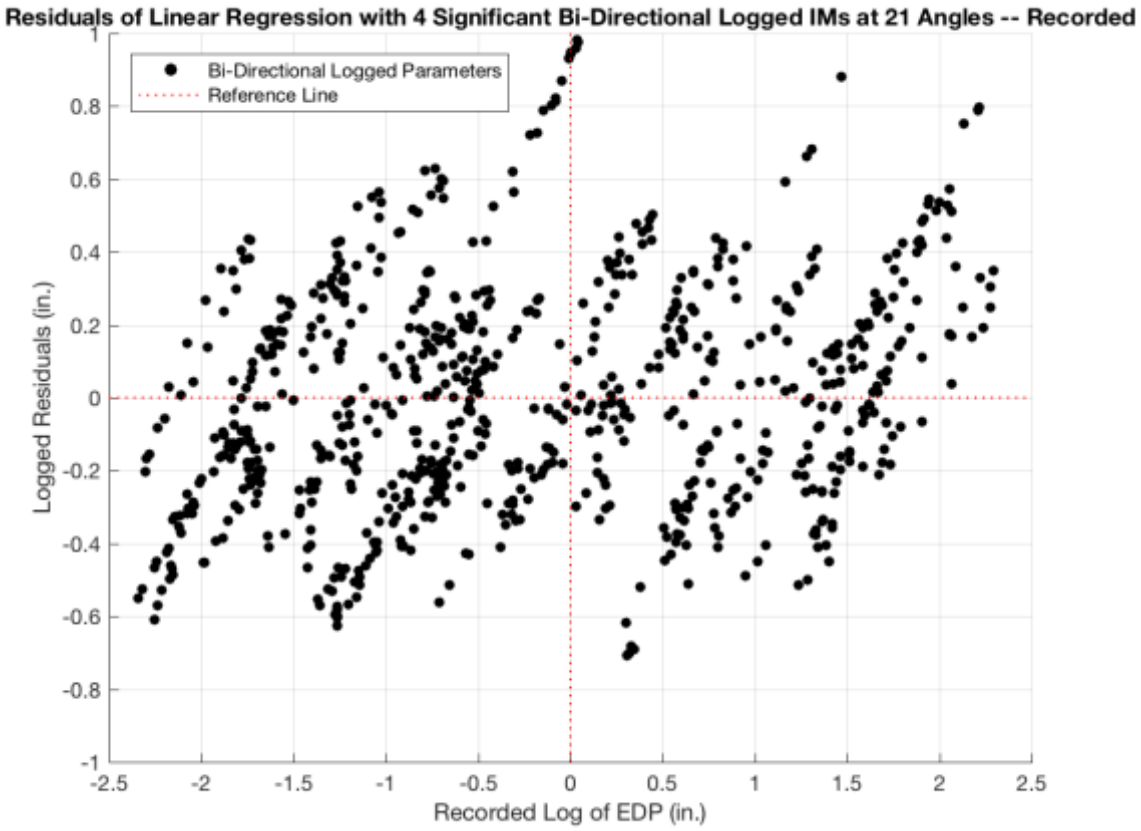

Figure 17: Residuals of logged recorded linear regression considering Angles 0° to 180°

There is clearly a trend in the residuals for the recorded set in the combination of the orthogonal components and the incorporation of 21 ground motions angles ranging from 0 to 180 degrees at 9 degree increments. The regression consistently overestimates the EDP compared to the actual EDP of the bridge by about 1.5 inches. The graphs on the following page show the recorded data against the simulated data for all simulation methodologies. The values are in the logged domain and each line represents the best fit line of one simulation realizations and one recorded ground motion for that specific angle of rotation.

3.6.1 Arias Intensity

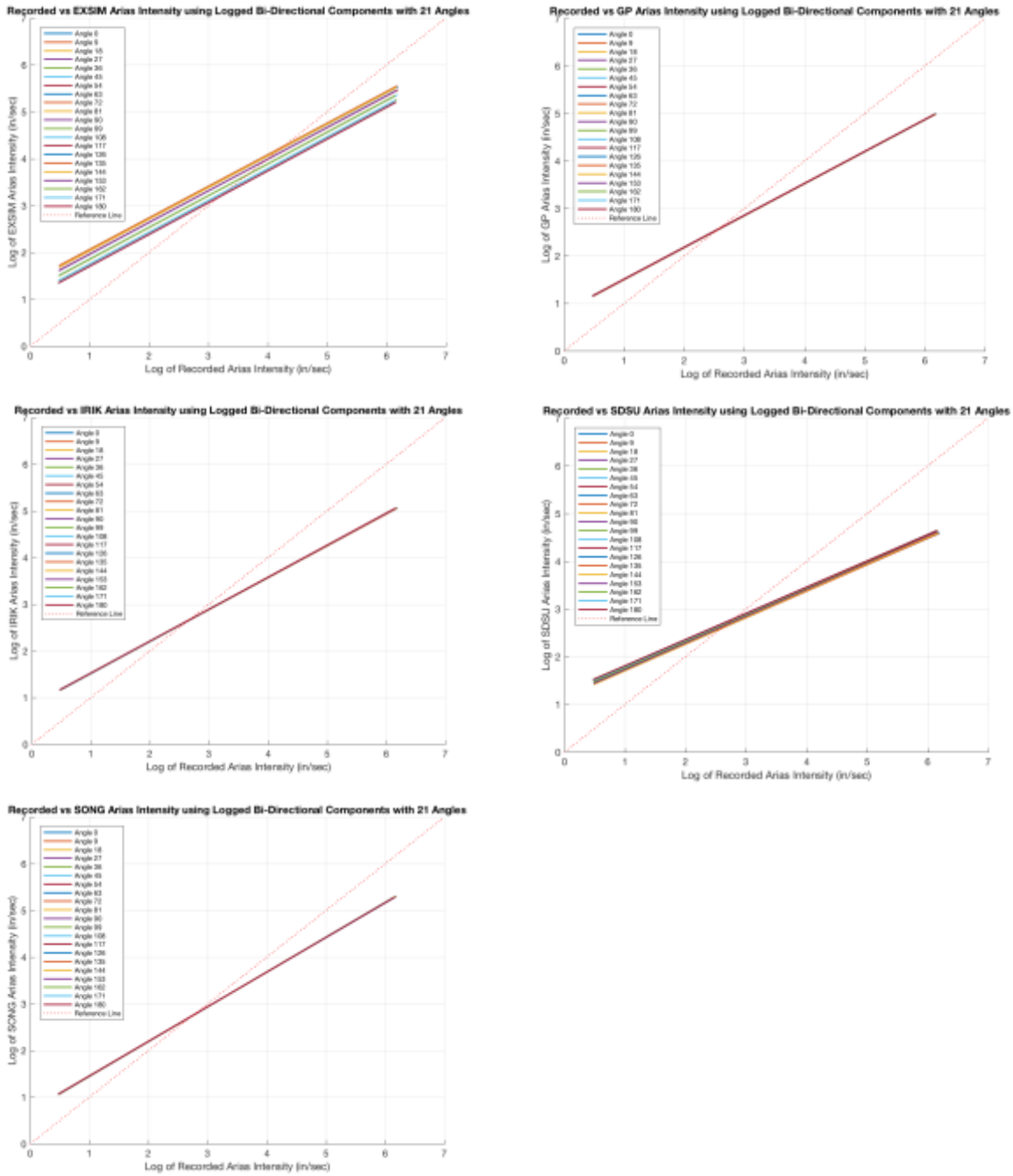

Figure 18: Recorded vs. Simulated Arias Intensity at angles of GM rotation from 0˚ to 180˚

For a majority of the simulation methodologies, the angle of rotation had negligible effect on the relationship between the Arias Intensity of the simulated time histories and the recorded ground motions. EXSIM, and to a lesser extent, SDSU, due possess more variation in the data than the other methodologies. In the EXSIM graph, as the angles rotated from 0˚ to 180˚, the larger angles of rotation produced the same results as the smaller angles; that is to say, the larger angles from 135˚ to 180˚ produced data so similar to the angles below 130˚ that these results overwrote the

plot lines from the smaller angles. As the angle increased from 135˚ to 180˚, the simulated Arias Intensity decreased. While the actual values of the Arias Intensities varied with angle of rotation, the relationship, or the slope of the lines, remained the same.

3.6.2 Significant Duration

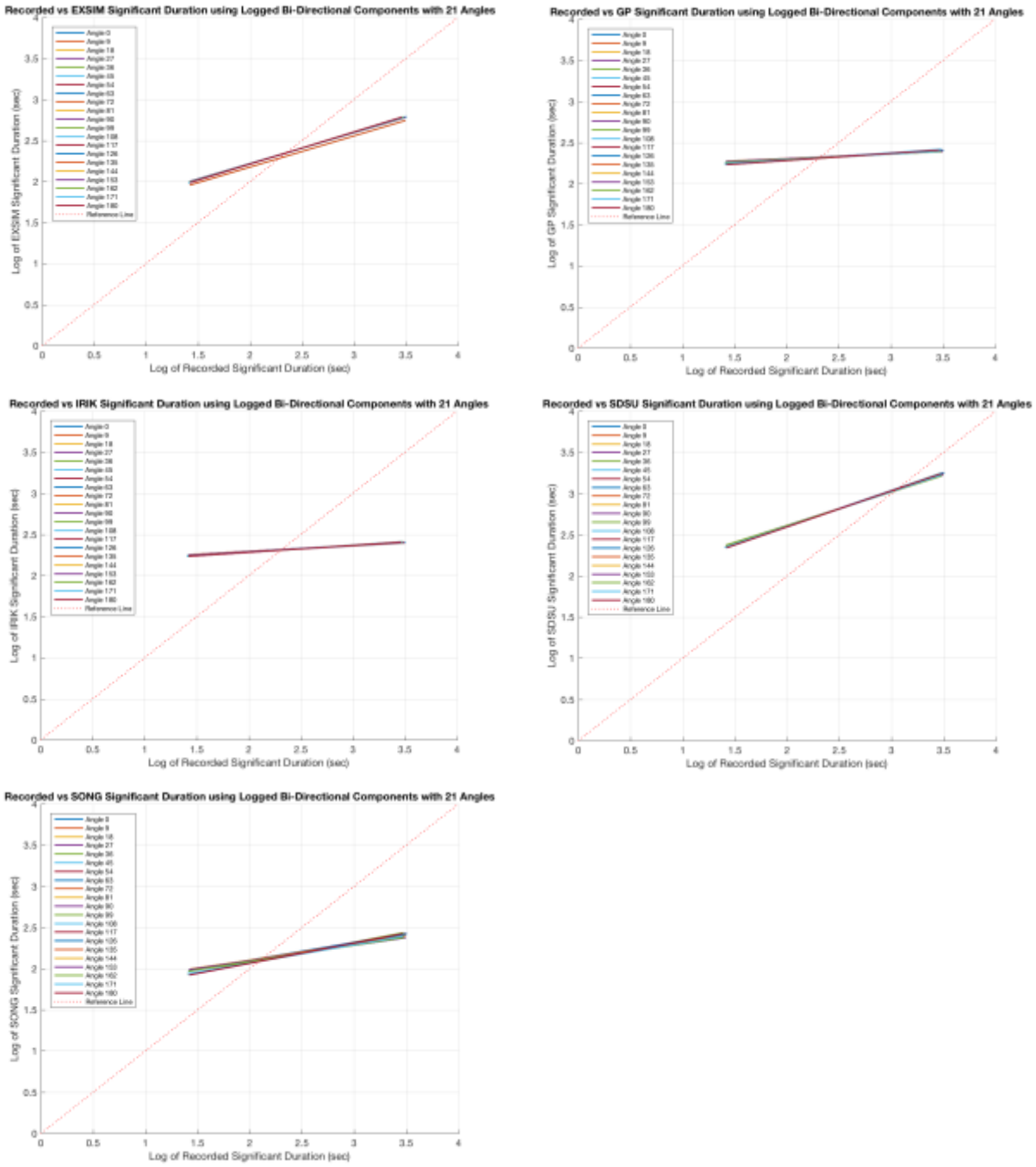

Figure 19: Recorded vs. Simulated T_d at angles of GM rotation from 0˚ to 180˚

Significant Duration had a weak relationship between the simulation methodologies and the recordings. EXSIM and SDSU exhibited positive trends but both methodologies produced

simulations that overestimated the Significant Duration of the recordings until the parameter reached 12 seconds. A trend seen in all the IMs and EDP of the Recorded vs. Simulated graphs is the simulations overestimate the recordings in their respective parameters until a threshold value is reached. Once that threshold value has been reached, i.e. 12 seconds for Significant Duration, the simulations begin to underestimate the parameters with respect to the recordings.

3.6.3 Slope of the Predominant Frequency

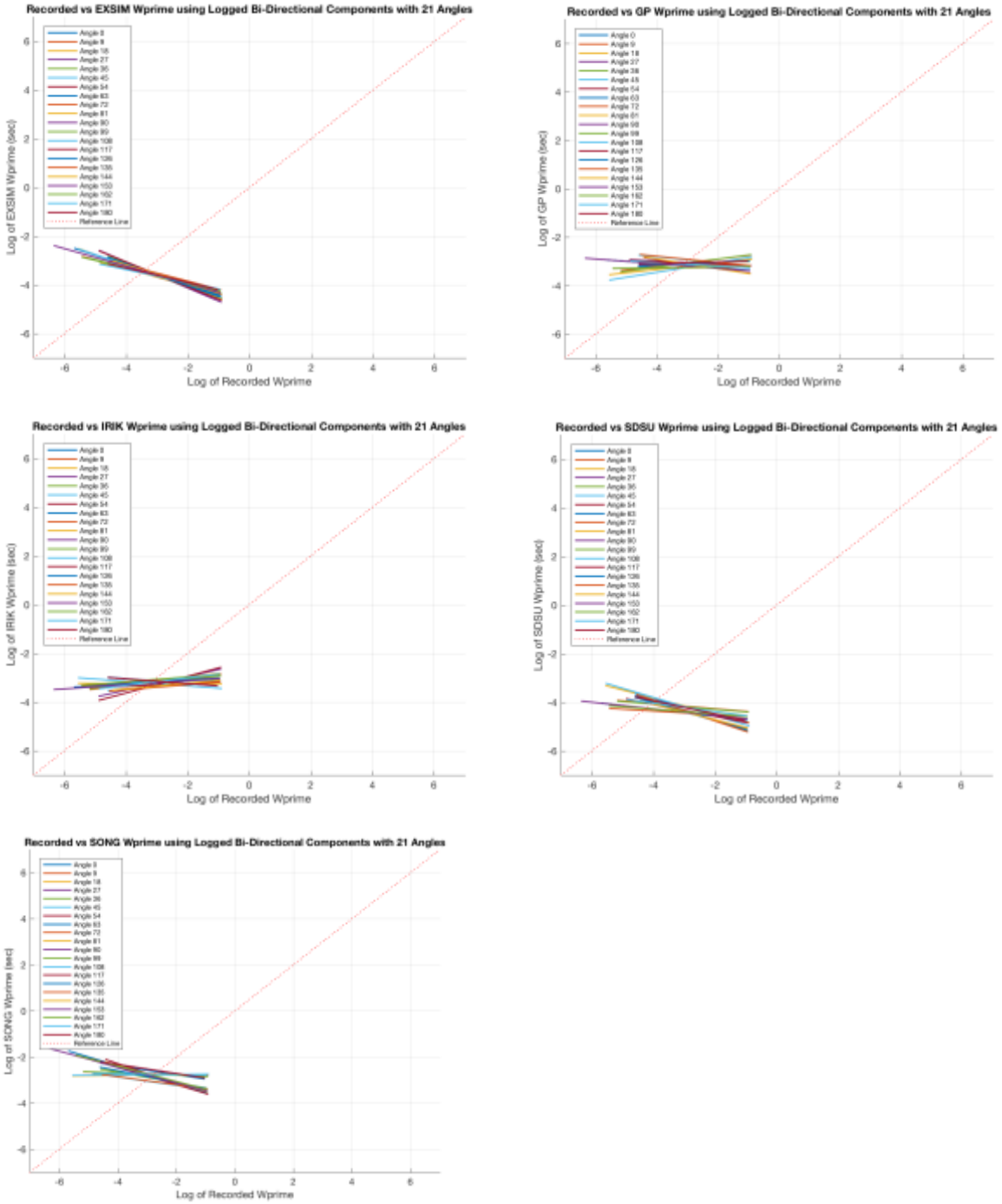

Figure 20: Recorded vs. Simulated ω' at angles of gm rotation from 0˚ to 180˚

For most simulation methodologies, ω' was not significant and did not yield any meaningful results when incorporated into the regression. Ω' was slightly significant for the regression of the recorded data set but it did not significantly contribute to the estimation of the EDP in the simulated methodologies of EXSIM, GP, and IRIK. There is a trend seen in EXSIM and a slight trend in SDSU but ω' was not significant in the linear regression of the logged results of EXSIM. A threshold value was also seen here which was inherent in all the simulation methodologies; once the simulated ω' reached a threshold value of 0.022, the simulations switched from overestimating the recordings to underestimating them. As displayed in the results in Appendix A.3.5, ω' was extremely significant in SDSU and SONG but had no significance with the other three simulation methodologies.

Figure 20, in Section 4.6.4, on the following page depicts the recorded vs. simulated graphs for the different simulation methodologies with the significant intensity measure of predominant frequency at mid duration. This intensity measure was measured as the slope of the cumulative level-up crossings of the time-history at the point of which the Significant Duration had reached half of its duration. In other words, the point of interest is at the time in which half of the energy produced by the ground motion had been accumulated. There was little variation in the predominant frequency at mid duration (ω_{mid}) with respect to the angle of rotation for the ground motion. The threshold value for the simulated motions with this intensity measure was around 5; once the threshold value had been reached, the simulations interchanged from underestimating the recorded ω_{mid} to overestimating its recorded counterpart. As displayed in the figure below, all simulation methodologies produced similar results and followed similar trends.

3.6.4 Predominant Frequency at Mid Duration

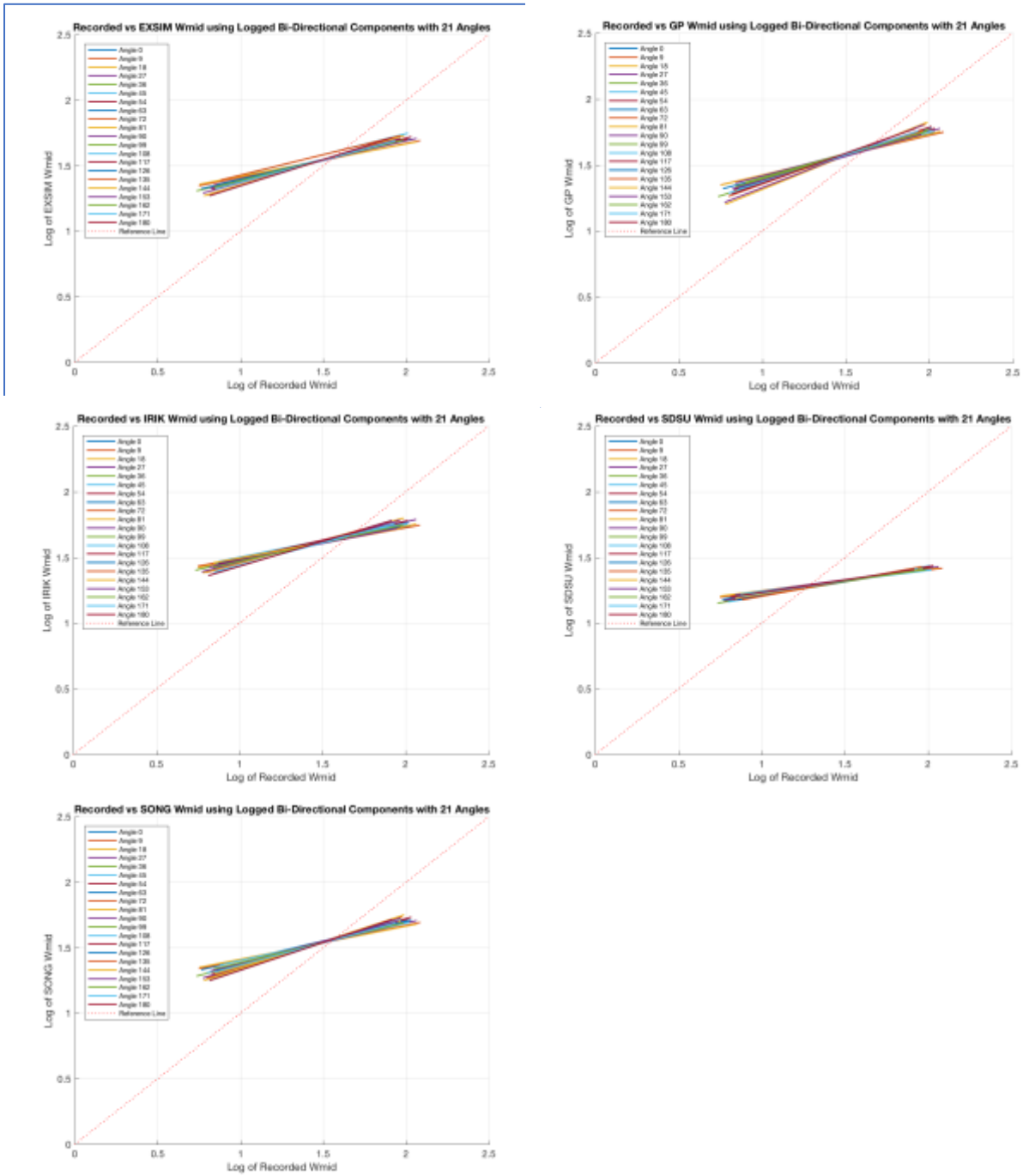

Figure 21: Recorded vs. Simulated ω_{mid} at angles of GM rotation from 0˚ to 180˚

Figure 22, in Section 4.6.5, illustrates the recorded vs. simulated graphs for the bridge's EDP. The results from plotting EDP for different attack angles of recorded to simulated EDP provided enlightening insight. Dispersion is highest with EXSIM and SDSU but most pronounced in EXSIM. This is expected, given the dispersion seen in the EXSIM IMs, specifically, Arias Intensity. The fact that the slope of the best fit lines change as the angle of rotation changes is noteworthy.

3.6.5 Engineering Demand Parameter

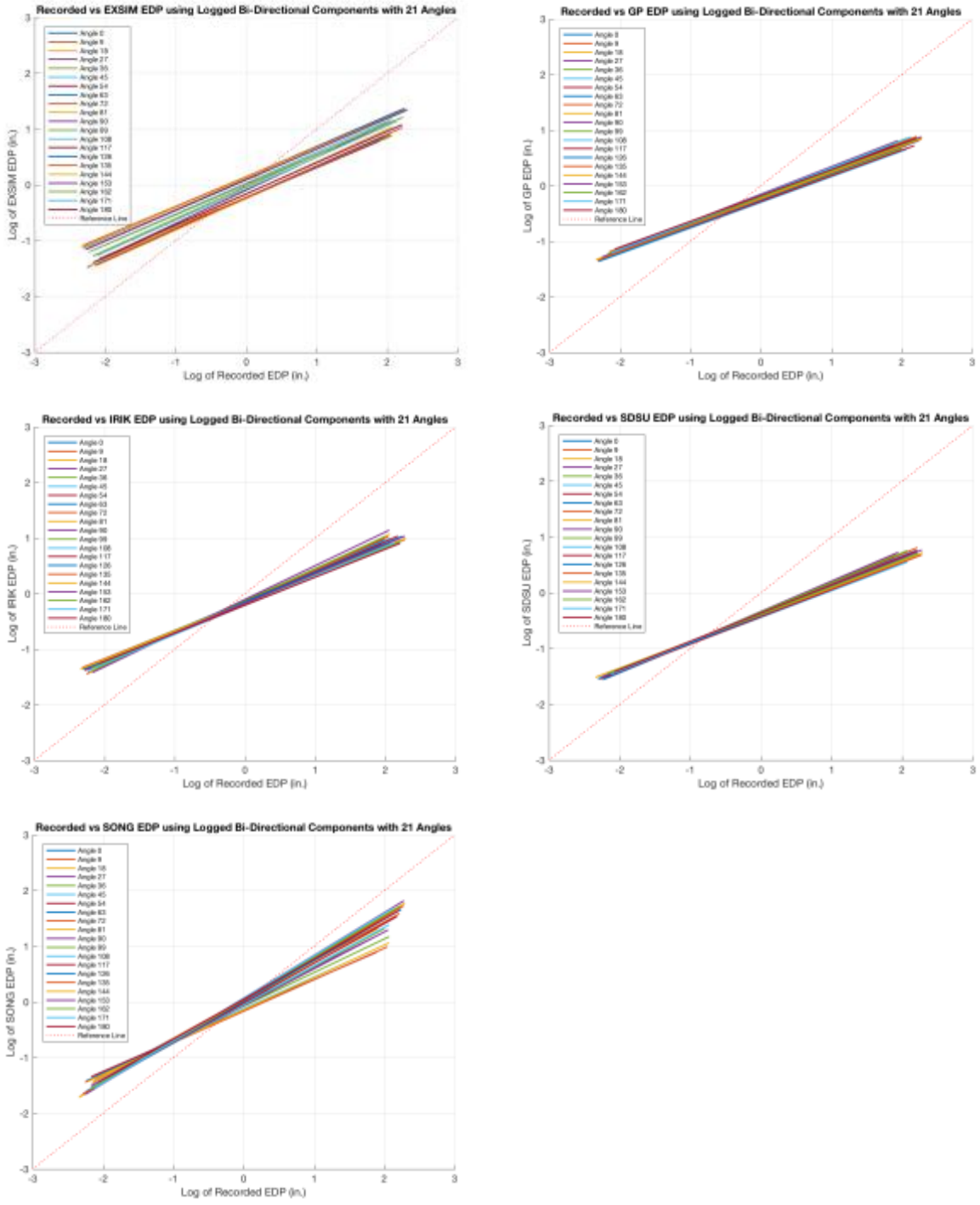

Figure 22: Recorded vs. Simulated EDP at angles of GM rotation from 0˚ to 180˚

This change in slope was not seen in the intensity measures; however, the mixed effects regression, elaborated on in Section 4.7, shows that the angle of rotation does have an effect on the EDP of the bridge and the relationship between the recorded and simulated EDP counterpart changes based on the angle. This most prominent change is in the simulation

methodology of EXSIM, which is understandable given that EXSIM orthogonal components are identical to each other; a larger effect is seen in EXSIM because the simulation methodology produces identical orthogonal acceleration records. The two graphs below show the Arias Intensity graph of EXSIM compared to the EDP graph of EXSIM. The different values the angle of rotation produces with the Arias Intensity correlate with the different responses the bridge sees with its EDP.

3.7 Mixed Effects Regression

As previously discussed, a mixed effects regression model of the logged intensity measures and EDP was executed to examine the effects ground motion station (distance from the hypocenter), simulation run, and the ground motion angle of rotation have on the ability of the intensity measures to estimate the bridge's EDP. Intensity measures and EDPs that were used reflected bi-directional components per the previously mentioned methodology in Section 4.5. Results obtained due to the mixed effect of simulation run are displayed below.

3.7.1 Random Intercept

The following are the random intercepts considered during the mixed effects regression:

1. Ground Motion Station (i.e. gm)
2. Simulation Run (i.e. sim)
3. Angle of Rotation (i.e. ang)

The preliminary recorded equation for the mixed effects regression with three random intercepts is presented below. "R" denotes recorded data was used.

$$Ln(EDP^R) = a_o^R + a_{gm}^R + a_{ang}^R + b_1^R x_{Ia}^R + b_2^R x_D^R + b_3^R x_{wmid}^R + b_4^R x_D^R + b_5^R x_{w'}^R + b_6^R x_{Ia}^R x_{wmid}^R + b_7^R x_D^R x_{wmid}^R + b_8^R x_{Ia}^R x_{wmid}^R + b_9^R x_{Ia}^R x_{w'}^R + b_{10}^R x_D^R x_{w'}^R + b_8^R x_{w'}^R x_{wmid}^R + \varepsilon_1$$

The preliminary simulated equations for the mixed effects regression with three random intercepts is presented below. "S" denotes simulated data (EXSIM, GP, IRIK, SDSU, and SONG). All simulated methodologies were characterized in this way.

$$Ln(EDP^S) = a_o^S + a_{gm}^S + a_{ang}^S + b_1^S x_{Ia}^S + b_2^S x_D^S + b_3^S x_{wmid}^S + b_4^S x_D^S + b_5^S x_{w'}^S + b_6^S x_{Ia}^S x_{wmid}^S + b_7^S x_D^S x_{wmid}^S + b_8^S x_{Ia}^S x_{wmid}^S + b_9^S x_{Ia}^S x_{w'}^S + b_{10}^S x_D^S x_{w'}^S + b_8^S x_{w'}^S x_{wmid}^S + \varepsilon_1$$

Table 13 on the following page demonstrates the random effects the ground motion station, the simulation run, and the angle of rotation produced on the fixed intercept estimates for the recorded data as well as the five simulation methodologies.

Ground Motion Type	Ground Motion Station	Simulation Run	Angle of Rotation
Recorded	Large Effect	N/A	Small Effect
EXSIM	Large Effect	No Effect	Significant Effect
GP	Large Effect	Negligible Effect	Negligible Effect
IRIK	Large Effect	Negligible Effect	Negligible Effect
SDSU	Significant Effect	Significant Effect	Significant Effect
SONG	Large Effect	Negligible Effect	Small Effect

Table 13: Mixed Effects regression results of logged parameters considering all angles

Given the results of the multiple effects regression, it was concluded that simulation realization had no effect on the results and thus, one simulation realization is sufficient to represent the specific methodology its derived from. For this reason, the data presented throughout this research incorporated only one simulation realization from each simulation methodology.

The angle of rotation had a small, almost negligible effect on the recorded ground motions. The angle of rotation only had a significant effect on the intercept estimate with EXSIM and SDSU; this is consistent with the plotted graphs with differing angles shown in Section 4.6. Ground motion station, and in particular, the distance the station's location resides from the hypocenter, had a large effect on the intercept of the regression and varied by about 2.5 inches depending on the station number. The results pertaining to the ground motion station were expected; there should be a correlation between the distance the records are taken at and the effect that these records produce on the intercept estimates for Arias Intensity, Significant Duration, the slope of the predominant frequency, and the predominant frequency at mid-duration. It is surprising, however, that the ground motion angle of rotation produced a small effect on the regression estimated for the recorded data set. It is notable that the simulations, save for SDSU, were able to replicate this characteristic and bodes well for their resilience against tests of comparison. The ground motion station was the only random effect taken into account for the revised mixed effects regression.

3.7.2 Random Intercept and Random Slope

An analysis of the significance of random slope effects was also performed. The three effects (gm, sim, and ang) were considered as both random intercepts and random slopes; however, the results yielded an un-converging model. There was no convergence upon considering the effect of the random slopes for either ground motion station, simulation realization, or angle. Different variations of incorporating random slope were also considered (i.e., using one random slope such as ground motion station) but the model would not converge. Thus, the revised model used subsequently consisted of one simulation realization with the ground motion station as the only random effect considered.

3.8 Statistical Comparison Between Recorded and Simulated Distributions

For the final stage of the analysis, the statistical distributions of the recorded and simulated data were compared to one another. The mean and standard deviation of the recorded and simulated data are shown below in Table 14.

Ground Motion Type	**Parameter**	**Mean**	**Standard Deviation**
Recorded	I_a	3.14	1.60
	T_d	2.43	0.48
	ω'	-2.65	0.78
	ω_{mid}	1.43	0.27
	EDP	-0.24	1.21
EXSIM	I_a	3.34	1.22
	T_d	2.38	0.27
	ω'	-3.74	1.26
	ω_{mid}	1.52	0.19
	EDP	-0.23	0.80
GP	I_a	2.95	1.35
	T_d	2.32	0.16
	ω'	-3.11	-0.88
	ω_{mid}	1.55	0.20
	EDP	-0.33	0.74
IRIK	I_a	2.98	1.27
	T_d	2.32	0.27
	ω'	-3.18	0.78
	ω_{mid}	1.59	0.16
	EDP	-0.29	0.82
SDSU	I_a	2.94	1.33
	T_d	2.79	0.30
	ω'	-4.39	0.83
	ω_{mid}	1.31	0.11
	EDP	-0.51	0.89
SONG	I_a	3.04	1.39
	T_d	2.18	0.25
	ω'	-2.84	0.96
	ω_{mid}	1.52	0.21
	EDP	-0.19	1.00

Table 14: Distribution means and standard deviations for recorded and simulations

The actual values of the intensity measures do not necessarily have to be identical but the distributions between the recorded and its simulated counterparts must be similar so that they can confidently be used interchangeably.

All data for this section uses logged intensity measures and EDP that have combined the orthogonal components. All angles between 0 and 180 at 9˚ increments have been included. The intensity measures used are the ones that were significant in the recorded data set when considering all angles. Only one simulation realization was considered for each simulation methodology since simulation run was found to have no effect. The distributions for the recorded and each of the simulations for each significant intensity measure and EDP are graphed below in Figure 23. All values are logged and all angles are considered.

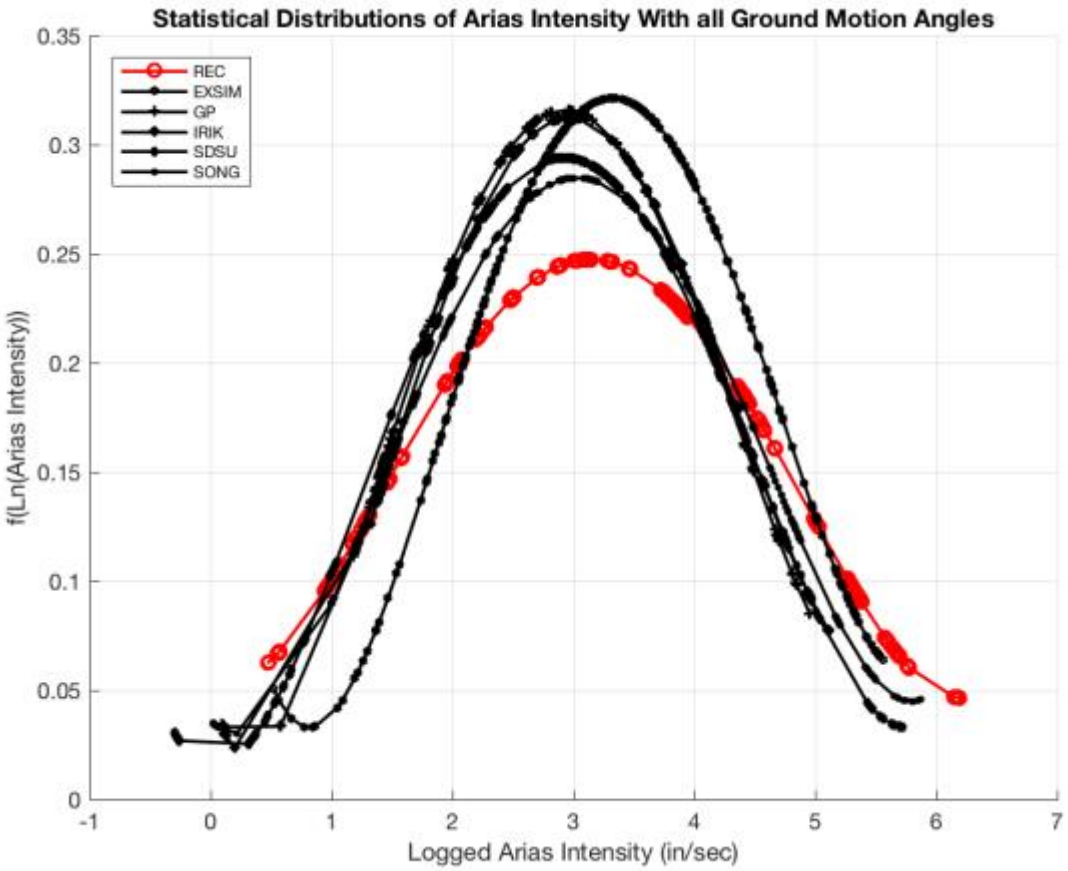

Figure 23 (a): I_A Probability dISTRIBUTION Considering angles from 0˚ to 180˚

The mean and standard deviations for Arias Intensity and EDP proved to be incredibly similar between all simulation methodologies and their recorded counterpart. IRIK and EXSIM were able to most accurately capture the mean and standard deviation of the recorded significant duration while SDSU and SONG were off in their distributions.

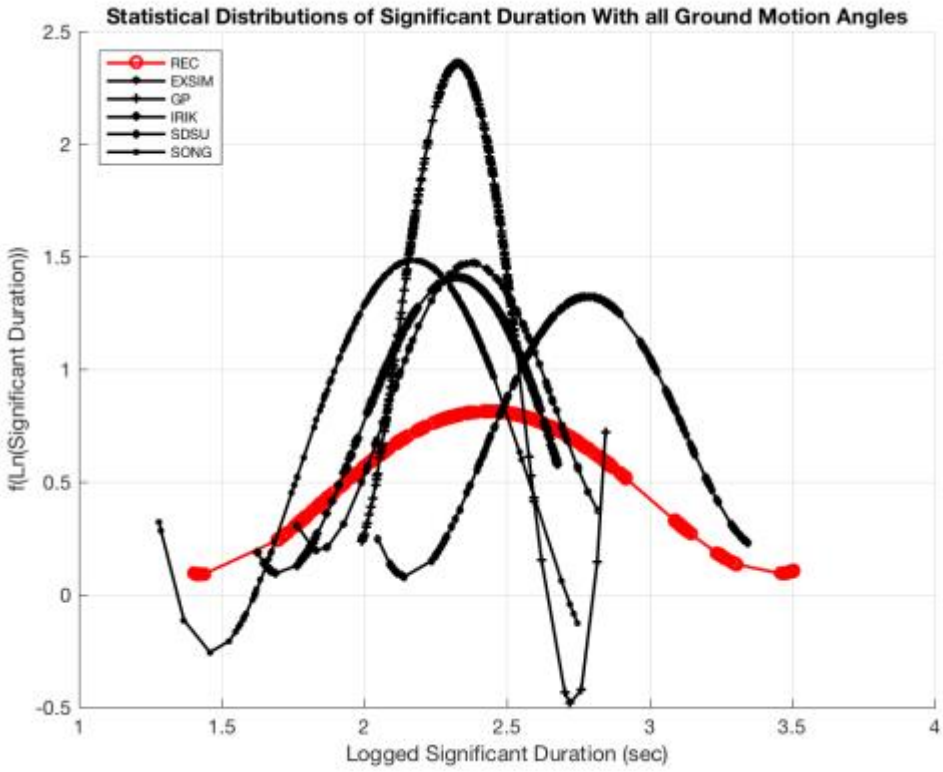

Figure 23 (b): T_d Probability distributions considering angles from 0˚ to 180˚

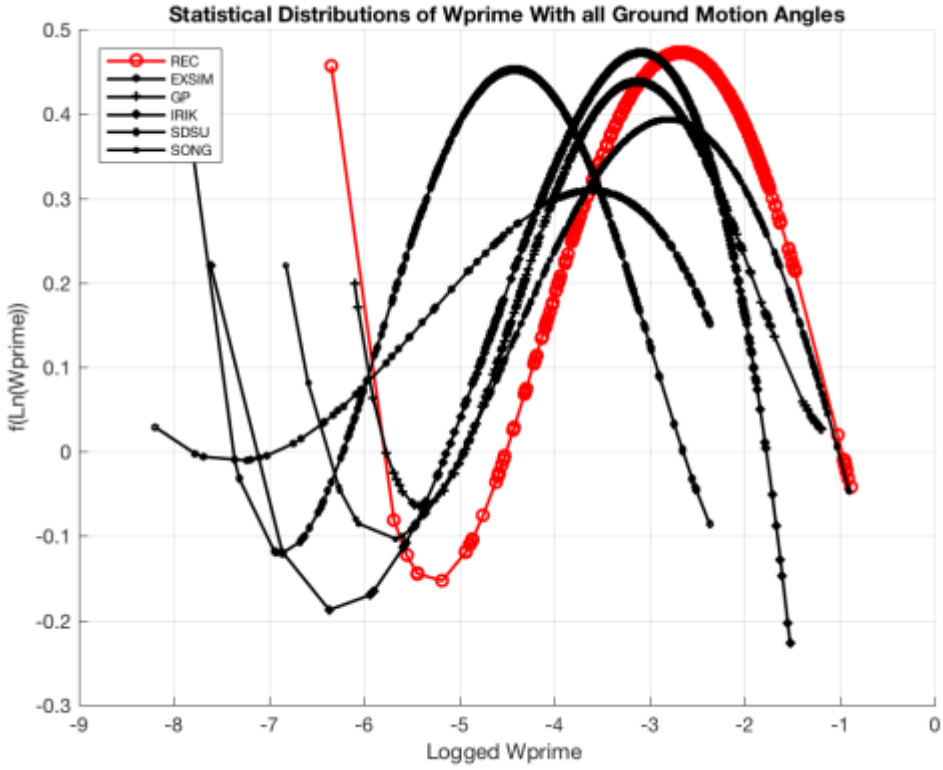

Figure 23 (C): ω′ Probability distributions considering angles from 0˚ to 180˚

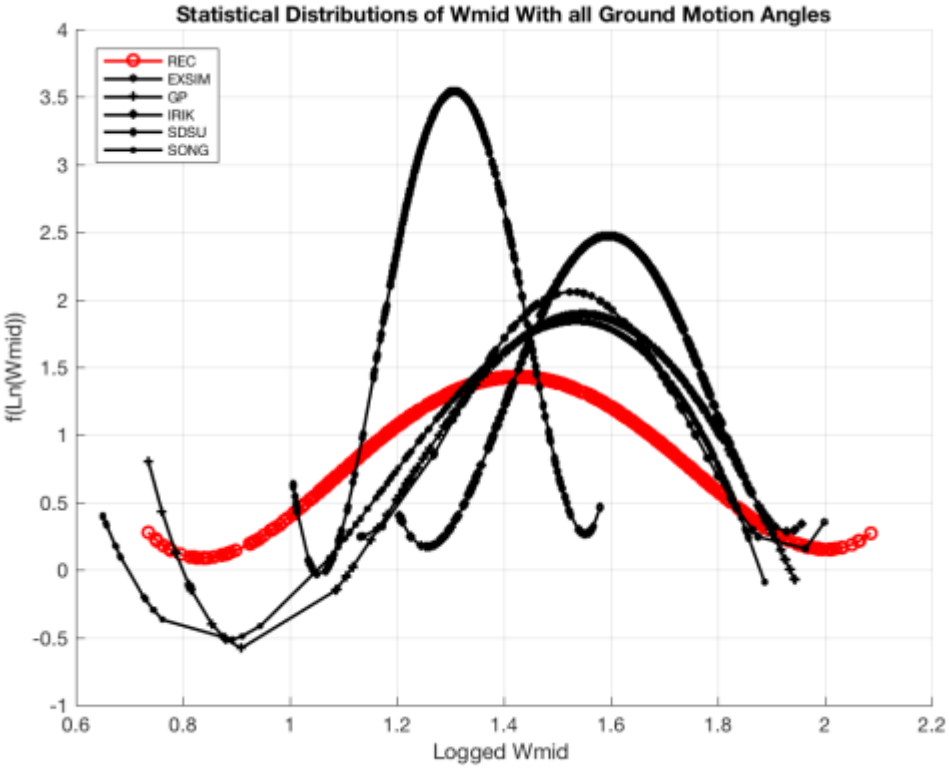

Figure 23 (D): ω_{mid} Probability distributions considering angles from 0˚ to 180˚

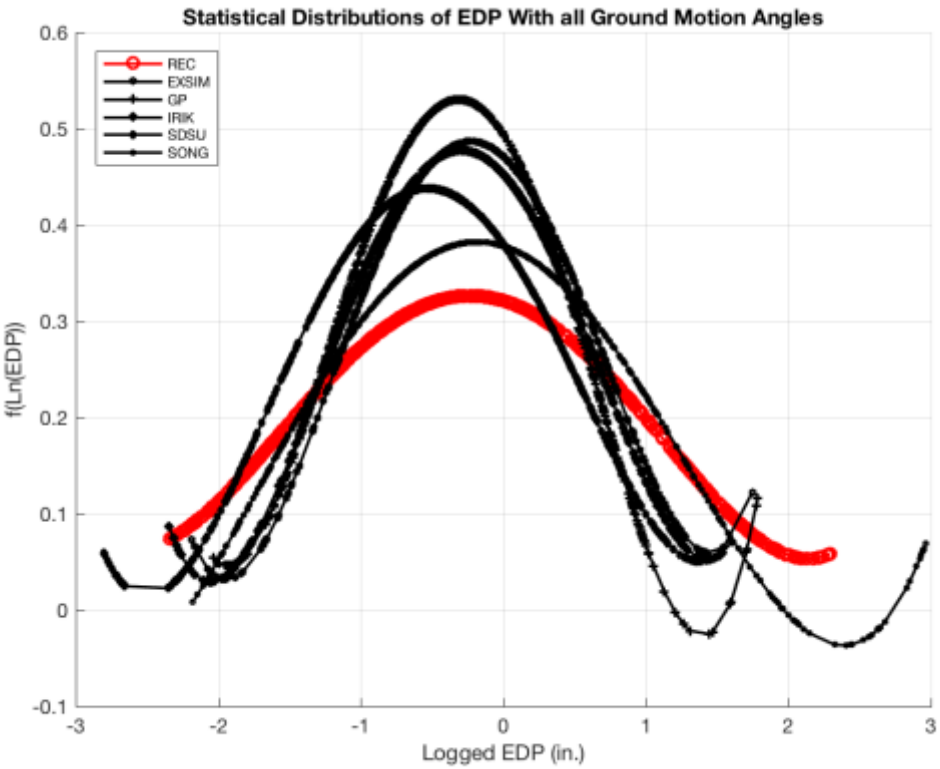

Figure 23 (E): edp Probability distributions considering angles from 0˚ to 180˚

All simulations were unable to simulate ω' efficiently in terms of mean when compared to the recorded. EXSIM, which was the simulation in which ω' was incredibly significant did not possess a similar distribution to the recorded ω' distribution.

ω_{mid}, also a significant parameter in the recorded and simulated data sets, was unable to be accurately captured by the simulations in terms of their mean and standard deviation in relation to the recorded data.

Despite differences in distribution for ω' and ω_{mid}, and somewhat for Significant Duration, the distribution of the EDP are considerably similar between recorded and all simulation methodologies. Their means and standard deviations provide for meaningful comparisons. Furthermore, the simulations performed relatively similar to one another in terms of their EDP distributions; that is to say, simulation methodologies produced the similar performance in the bridge between each other. Despite their differences, the simulated intensity measures were able to simulate a corresponding behavior in the bridge similar to that seen with the recorded data set.

To further assess the data, a hypothesis test was performed on the means EDP between the simulated and the recorded data sets. Due to the discrepancy in variance between the simulated and recorded parameters, a two-tail Aspin-Welch (Welch 1938) was considered with a null hypothesis assuming the mean of the engineering demand parameters to be equal to those of the recorded. The alternative hypothesis, considered to be true if the resultant p-value of the Aspin-Welch test proves to be less than the threshold value of 0.05, is that the true difference in the means of the recorded and simulated data sets cannot be taken as 0. This test is incorporated to see if means from two populations are equivalent. The test statistic used in the hypothesis test is shown below per (Galasso, et al. 2013); z_x and z_y are sample means, s_x and s_y are the sample standard deviations, and m and n are the sample sizes.

$$t = \frac{z_x - z_y}{\sqrt{\frac{s_x^2}{n} + \frac{s_y^2}{m}}}$$

The sample means and standard deviations are provided in Table 14 and the sample size for all populations is 798, which includes 38 ground motion stations at 21 incremental ground motion attack angles. Table 15 summarizes the t values acquired from testing the recorded EDPs against the simulated EDPs for each simulation methodology and the p-value acquired from the Aspin-Welch test administered in Rstudio. The Aspin-Welch test performed on simulation methodologies, EXSIM, IRIK, and SONG accepted the null hypothesis with p-values greater than the threshold 0.05. It is concluded that for the mean of the recorded EDP is statistically similar to the means of the EXSIM, IRIK, and SONG EDP. GP and SDSU simulation methodologies rejected the null hypothesis and, thus, the mean of their EDPs are not significantly similar to the mean of the recorded EDP data set.

Ground Motion Type	Test Statistic	P-value	Satisfied Null Hypothesis
EXSIM	-0.341	0.734	Yes
GP	-5.681	1.88E-08	No
IRIK	0.947	0.344	Yes
SDSU	5.009	6.14E-07	No
SONG	-0.962	0.336	Yes

Table 15: Aspin-Welch t-test on recorded and simulated data sets for EDP

Given the difference in the actual values of the EDP means between the recorded data set and the GP and SDSU data set, it is understandable that the means of the EDP are not significantly similar to the recorded EDP.

CHAPTER 5: Summary and Conclusions

Simulations, for the most part, performed similarly to each other; exceptions to that occurrence were realized in EXSIM and SDSU data sets when comparing Arias Intensity, Significant Duration, ω_{mid} and EDP to the recorded data. All simulation methodologies were unable to drive the bridge to experience plasticity as the recorded ground motions were able to accomplish.

Linear regressions were performed on raw intensity measures and EDP for recorded and all simulated methodologies. Raw intensity measures produced residuals with a considerable trend as the EDP increased. The solution to this problem performed a linear regression in the logarithmic domain, which produced residuals with no significant trend. The logarithmic domain of the recorded parameters also produced a linear regression which was able to accurately capture 94% of the variance in the mean of the drift of Node 12 by the three intensity measures, Arias Intensity, Significant Duration, and predominant frequency at mid duration. The bias was not significant and the three significant intensity measures increased in significance when assumed a lognormal distribution. It was concluded that a logarithmic presentation of the recorded regression suited the objectives of this research and so the same procedure was performed on the simulations.

A preliminary mixed effects regression was performed on each of the simulation methodologies to assess the effect that simulation run (realization) had on the fixed effect intercept estimates. The results from the mixed effects regression showed that the realization did not have effect on the intercept estimates; it was concluded that the use of one simulation realization was appropriate and all subsequent regression runs used a single simulation realization in comparison to its recorded counterpart.

Because the intensity measures each have a different characterizing distribution, transformations were performed to the standard normal domain according to their respective distributions. Transformation were done using the methodology expressed in PEER Report 2010/02 (Rezaeian and Der Kiureghian 2010). Results from the regression performed with the Rezaeian transformed parameters were not as robust as expected and the variables used in subsequent analysis were in the logarithmic domain.

Due to the EDP being the SRSS of the maximum column drift, it was deemed more conducive to the regression model to provide a means to combine the x and y components for the intensity measures. To combine the orthogonal components of the ground motions in accordance with the respective intensity measures, the SRSS of the Arias Intensity was used and the geometric mean of Significant Duration, and the predominant frequency at mid duration was taken. A linear regression of the log of these combined intensity measures and their corresponding EDPs was performed. All simulation methodologies tended to overestimate the intensity measures and EDPs until a certain threshold value was achieved at which point, the simulations began to underestimate when compared to the recorded. It was noteworthy that the threshold value of the simulations, at which they switched from underestimating to overestimating their recorded counterpart, was the same number across all simulation methodologies.

The angle of rotation at which the ground motions were applied to the bridge was also taken into consideration. Ground motions were rotated at 9 degree increments from 0˚ to 180˚. A linear regression of the logged variables considering all angles mentioned previously was performed. When the angle of ground motion rotation was considered, the regression results revealed that the slope of the predominant frequency (ω') was a significant parameter. This model with the ground motions rotated at 9 degree increments and including ω' as a parameter in the regression was performed for all simulation methodologies.

A complete mixed effects regression was performed on the recorded and simulated data sets. Ground motion station, simulation realization, and angle of rotation were considered random effects. As previously stated, simulation realization had no effect on the fixed effects intercept estimates. The angle of ground motion rotation influenced the intercept of the recorded, EXSIM, and SDSU data but did not do so considerably. Ground motion station always had a considerable effect on both recordings and all simulations, which was expected.

Simulated intensity measures were able to produce similar distributions in Arias Intensity and Significant Duration when compared to the recorded. Despite their differences in ω' and ω_{mid}, the simulated intensity measures were able to simulate a corresponding behavior in terms of maximum drift of column Node 12 in the bridge similar to that seen with the recorded data set. An Aspin-Welch test was performed in Rstudio to assess the similarity between the two populations of recorded and simulated data sets. The parameter in consideration was the mean of the EDPs and it's similarity between the recorded EDP and the simulated EDP. It was concluded that the means of the EXSIM, IRIK, and SONG EDP data set were significantly similar to the mean of the recorded EDP. The null hypothesis of equality of EDP means between these simulated methodologies and the recorded data was accepted. More research is encouraged in the future to assess the validity of the use ground motion simulations in lieu of or as a supplement to recorded ground motions. It is concluded here that simulated motions may be a very powerful tool in the statistical behavioral analysis of bridges.

REFERENCES

Bozorgnia, Y., and V. V. Bertero. 2004. *Earthquake Engineering: From Engineering Seismology to Performance-Based Engineering* (CRC Press).

Campbell, KW, and Y Borzorgnia. 2008. "NGA ground motion model for the geometric mean horizontal component of PGA, PGV, PGD, and 5% damped linear elastic response spectra for periods ranging from 0.01 to 10s." *Earthquake Spectra* 24 (1): 139-171.

Galasso, Carmine, Peng Zhong, Farzin Zareian, Iunio Iervolino, and Robert W. Graves. 2013. "Validation of ground-motion simulations for histrorial events using MDoF systems." *Earthquake Engineering and Structural Dynamics* (Wiley Online Library) 42: 1395-1412.

2017. *GMSV_17_3/NR.* March 6. Accessed 2017. http://hypocenter.usc.edu/bbp/GMSV_17_3/NR/input_files/nr_v13_3_1.stl.

Graves, RW, and A Pitarka. 2010. "Broadband ground-motion simulation using a hybrid approach." *Bulletin of Seismological Society of America* 100 (5A): 54-60.

Mobasher, Bahareh. 2016. "Quatification of Bridge Performance Variability due to Modeling Uncertainties ." PhD Dissertation, Department of Civil and Environmental Engineering, University of California, Irvine, Irvine.

Rezaeian, S., and A. Der Kiureghian. 2010. *Stochastic Modeling and Simulation of Ground Motions for Performance-Based Earthquake Engineering.* Department of Civil and Environmental Engineering, Univeristy of California, Berkeley, Berkeley: Pacific Earthqauke Engineering Research Center.

Rezaeian, Sanaz, Zhong Peng, Stephen Hartzell, and Farzin Zareian. 2015. "Validation of Simulated Earthquake Ground Motions Based on Evolution of Intensity and Frequency Content." *Bulletin of the Seismological Society of America* 105 (6).

Scott, M.H., and G.L. Fenves. 2006. "Plastic Hinge Integration Methods for Force-Based Beam-Column Elements." *Journal of Structural Engineering* (ASCE) 132 (2): 244-252.

Somerville, P., N. Collins, N. Abrahamson, R. Graves, and C. Saikia. 2001. "Ground motion attenuation relations for the central and eastern United States: Final Report." Report to U.S. Geol. Surv for Award 99HQGR0098, 38.

Welch, BL. 1938. "The significance of the difference between two means when the popluation variances are unequal." *Biometrika* 29: 350-362.

APPENDIX A: Linear Regression Results

A.1 Ground Motion Station Number Assignments

Station Abbreviation	Station Number
2033-ACI	1
2023-ANA	2
2027-ATB	3
2029-CAS	4
2036-FEA	5
2028-FIG	6
2021-FLE	7
2011-GLE	8
2016-H12	9
2004-JGB	10
2018-KAT	11
2039-LAN	12
2034-LBC	13
2032-LBR	14
2005-LDM	15
2013-LOS	16
2026-LV3	17
2035-MJH	18

Station Abbreviation	Station Number
2014-MU2	19
2020-NYA	20
2031-OAK	21
2006-PAC	22
2025-PEL	23
2022-PIC	24
2008-PKC	25
2007-PUL	26
2038-RMA	27
2019-RO3	28
2040-SBG	29
2001-SCE	30
2037-SEA	31
2010-SPV	32
2017-SSU	33
2002-SYL	34
2024-TPF	35
2015-TUJ	36
2030-VER	37
2012-WON	38

A.2 Intensity Measure Definitions

1. Normalized Arias Intensity (I_a)

Definition	X-Direction	Y-Direction	Combined Directions
$(\pi/2g)*\int a(t)^2dt$	I_{ax}	I_{ay}	I_a

2. Significant Duration (T_d)

Definition	X-Direction	Y-Direction	Combined Directions
Time elapsed between when the ground motion record has reached 5% and 95% of its Arias Intensity	T_{dx}	T_{dy}	T_d

3. Mid-duration (t_{mid})

Definition	X-Direction	Y-Direction	Combined Directions
Time at which half of the significant duration has occurred	t_{midx}	t_{midy}	t_{mid}

4. Rate of Energy accumulation (I_a/T_d)

Definition	X-Direction	Y-Direction	Combined Directions
$\frac{\text{Arias Intensity}}{\text{Significant Duration}}$	I_{ax}/T_{dx}	I_{ay}/T_{dy}	I_a/T_d

5. Slope of Predominant Frequency (ω')

Definition	X-Direction	Y-Direction	Combined Directions
The slope of the 2nd degree polynomial capturing instantaneous predominant frequency of the ground motion	ω_x'	ω_y'	ω'

6. Predominant Frequency at Mid-duration

Definition	X-Direction	Y-Direction	Combined Directions
The derivative of the best fit polynomial of the cumulative zero level-up crossings at mid duration	ω_{midx}	ω_{midy}	ω_{mid}

A.3 Linear Regression Results

A.3.1 Linear Regression given 5 IMs for the Y-directional components

IM	Slope Estimate	P-Value	Significance Level	R squared
Intercept (Bias)	4.0006	0.00325	**	0.7519
I_{Ay}	0.01876	2.4e-06	***	
D_y	-0.05518	0.39445		
T_{midy}	-0.05762	0.50397		
W'_y	0.43751	0.89011		
W_{midy}	-0.40119	0.03351	*	

A.3.2. Linear Regression given 3 IMs for the Y-directional components

IM	Slope Estimate	P-Value	Significance Level	R squared
Intercept (Bias)	3.7304	0.00329	**	0.7463
I_{Ay}	0.0194	4.64e-07	***	
D_y	-0.0941	0.01613	*	
W_{midy}	-0.3993	0.02699	*	

A.3.3.a Linear Regression of logged recorded data given 6 IMs for the X Direction

```
lm(formula = LogEDPRec ~ LogIaxRec + LogDurxRec + LogADxRec +
    LogTmidxRec + LogWprimexRec + LogWmidxRec, data = logREC)

Residuals:
     Min       1Q   Median       3Q      Max
-0.55067 -0.18520  0.02739  0.17447  0.73374

Coefficients: (1 not defined because of singularities)
              Estimate Std. Error t value Pr(>|t|)
(Intercept)    0.895536   1.086887   0.824  0.41607
LogIaxRec      0.593406   0.058965  10.064 1.94e-11 ***
LogDurxRec    -0.806989   0.297178  -2.716  0.01058 *
LogADxRec            NA         NA      NA       NA
LogTmidxRec    0.194687   0.330084   0.590  0.55946
LogWprimexRec  0.005918   0.077247   0.077  0.93941
LogWmidxRec   -0.890075   0.263773  -3.374  0.00195 **
---
Signif. codes:  0 '***' 0.001 '**' 0.01 '*' 0.05 '.' 0.1 ' ' 1

Residual standard error: 0.3176 on 32 degrees of freedom
Multiple R-squared:  0.9408,    Adjusted R-squared:  0.9316
F-statistic: 101.7 on 5 and 32 DF,  p-value: < 2.2e-16
```

A.3.3.b Linear Regression of logged recorded data given 6 IMs for the Y Direction

```
lm(formula = LogEDPRec ~ LogIayRec + LogDuryRec + LogADyRec +
    LogTmidyRec + LogWprimeyRec + LogWmidyRec, data = logREC)

Residuals:
     Min       1Q   Median       3Q      Max
-0.73551 -0.30086  0.00495  0.16788  0.97366

Coefficients: (1 not defined because of singularities)
              Estimate Std. Error t value Pr(>|t|)
(Intercept)    1.29581    1.35794   0.954   0.3471
LogIayRec      0.52177    0.07067   7.383 2.13e-08 ***
LogDuryRec    -0.61511    0.35696  -1.723   0.0945 .
LogADyRec           NA         NA      NA       NA
LogTmidyRec   -0.13486    0.43663  -0.309   0.7594
LogWprimeyRec  0.03926    0.11579   0.339   0.7368
LogWmidyRec   -0.66831    0.31010  -2.155   0.0388 *
---
Signif. codes:  0 '***' 0.001 '**' 0.01 '*' 0.05 '.' 0.1 ' ' 1

Residual standard error: 0.4159 on 32 degrees of freedom
Multiple R-squared:  0.8985,    Adjusted R-squared:  0.8827
F-statistic: 56.66 on 5 and 32 DF,  p-value: 5.87e-15
```

A.3.4.a Linear Regression of logged recorded data given 3 IMs for Y-direction components

IM	Slope Estimate	P-Value	Significance Level	R squared	Residual Error
Intercept	0.92232	0.35706		0.898	0.4045
Ln(I_{Ay})	0.52906	7.28e-10	***		
Ln(D_y)	-0.66854	0.00599	**		
Ln(W_{midy})	-0.62558	0.0344	*		

A.3.4.b Linear Regression of logged simulated data given 3 IMs for Y-direction component

IM	Slope Estimate	P-Value	Significance Level	R squared	Residual Error
Intercept	-1.373	<2e-16	***	0.9266	0.211
$Ln(I_{Ax})$	0.6007	<2e-16	***		
$Ln(D_x)$	-0.1804	2.17e-05	***		
$Ln(W_{midx})$	-0.2013	5.84e-06	***		

(EXSIM with one realization)

IM	Slope Estimate	P-Value	Significance Level	R squared	Residual Error
Intercept	-0.4323	0.0046	**	0.8632	0.307
$Ln(I_{Ax})$	0.5717	<2e-16	***		
$Ln(D_x)$	-0.2891	4.56e-08	***		
$Ln(W_{midx})$	-0.3908	5.89e-08	***		

(GP with one realization)

IM	Slope Estimate	P-Value	Significance Level	R squared	Residual Error
Intercept	-0.3059	0.0377	*	0.8476	0.3001
$Ln(I_{Ax})$	0.5543	<2e-16	***		
$Ln(D_x)$	-0.2479	3.57e-07	***		
$Ln(W_{midx})$	-0.4875	4.22e-11	***		

(IRIK with one realization)

IM	Slope Estimate	P-Value	Significance Level	R squared	Residual Error
Intercept	1.547	4.32e-06	***	0.7551	0.5034
$Ln(I_{Ax})$	0.4668	<2e-16	***		
$Ln(D_x)$	-0.8198	<2e-16	***		
$Ln(W_{midx})$	-0.6201	0.000293	***		

(SDSU with one realization)

IM	Slope Estimate	P-Value	Significance Level	R squared	Residual Error
Intercept	0.0951	0.509		0.8608	0.3273
$Ln(I_{Ax})$	0.6041	<2e-16	***		
$Ln(D_x)$	-0.4398	<2e-16	***		
$Ln(W_{midx})$	-0.53371	4.79e-13	***		

(SONG with one realization)

A.3.5 Linear Regression of logged simulated data given 4 IMs (All Angles)

IM	Slope Estimate	P-Value	Significance Level	R squared	Residual Error
Intercept	-0.5257	<2e-16	***	0.892	0.26
$Ln(I_A)$	0.5907	<2e-16	***		
Ln(D)	-0.3681	<2e-16	***		
Ln(W')	-0.00245	0.163			
$Ln(W_{mid})$	-0.5330	<2e-16	***		

(EXSIM with one realizations and 21 angles)

IM	Slope Estimate	P-Value	Significance Level	R squared	Residual Error
Intercept	-0.4478	<2e-16	***	0.9187	0.2347
$Ln(I_A)$	0.6146	<2e-16	***		
Ln(D)	-0.3842	<2e-16	***		
Ln(W')	0.000145	0.947			
$Ln(W_{mid})$	-0.5264	<2e-16	***		

(GP with one realizations and 21 angles)

IM	Slope Estimate	P-Value	Significance Level	R squared	Residual Error
Intercept	-0.3655	<2e-16	***	0.9103	0.2316
$Ln(I_A)$	0.6194	<2e-16	***		
Ln(D)	-0.3681	<2e-16	***		
Ln(W')	-0.00108	0.633			
$Ln(W_{mid})$	-0.5921	<2e-16	***		

(IRIK with one realizations and 21 angles)

IM	Slope Estimate	P-Value	Significance Level	R squared	Residual Error
Intercept	-1.034	<2e-16	***	0.942	0.244
$Ln(I_A)$	0.6116	<2e-16	***		
Ln(D)	-0.2751	<2e-16	***		
Ln(W')	-0.02104	<2e-16	***		
$Ln(W_{mid})$	-0.4762	<2e-16	***		

(SDSU with one realizations and 21 angles)

IM	Slope Estimate	P-Value	Significance Level	R squared	Residual Error
Intercept	-0.3518	<2e-16	***	0.911	0.2558
$Ln(I_A)$	0.6245	<2e-16	***		
Ln(D)	-0.5129	<2e-16	***		
Ln(W')	-0.0111	3.85e-06	***		
$Ln(W_{mid})$	-0.4304	<2e-16	***		

(SONG with one realizations and 21 angles)

APPENDIX B: Standard Normal Domain Transformation

IM	**Slope Estimate**		**P-Value**		**Significance Level**		**R squared**	
	NRT	RT	NRT	RT	NRT	RT	NRT	RT
Intercept	0.7283	-2.28e01	0.5347	0.00022		***	0.906	0.712
I_{Ay}	0.5766	3.993e-3	1.55e-10	0.00012	***	***		
D_y	-0.6390	-5.015e-1	0.0138	0.14677	*			
W_{midy}	-0.5532	-7.53e-1	0.0714	0.1009	.			
W'_y	0.0594	-4.25e-1	0.5942	0.23512				